INTERNATIONAL STANDARD

ISO 14222

Second edition
2022-03

Space environment (natural and artificial) — Earth's atmosphere from ground level upward

Environnement spatial (naturel et artificiel) — Haute atmosphère terrestre

Reference number
ISO 14222:2022(E)

ISO copyright office
CP 401 • Ch. de Blandonnet 8
CH-1214 Vernier, Geneva
Phone: +41 22 749 01 11
Email: copyright@iso.org
Website: www.iso.org

Published in Switzerland

Contents

Page

Foreword

ISO (the International Organization for Standardization) is a worldwide federation of national standards bodies (ISO member bodies). The work of preparing International Standards is normally carried out through ISO technical committees. Each member body interested in a subject for which a technical committee has been established has the right to be represented on that committee. International organizations, governmental and non-governmental, in liaison with ISO, also take part in the work. ISO collaborates closely with the International Electrotechnical Commission (IEC) on all matters of electrotechnical standardization.

The procedures used to develop this document and those intended for its further maintenance are described in the ISO/IEC Directives, Part 1. In particular, the different approval criteria needed for the different types of ISO documents should be noted. This document was drafted in accordance with the editorial rules of the ISO/IEC Directives, Part 2 (see www.iso.org/directives).

Attention is drawn to the possibility that some of the elements of this document may be the subject of patent rights. ISO shall not be held responsible for identifying any or all such patent rights. Details of any patent rights identified during the development of the document will be in the Introduction and/or on the ISO list of patent declarations received (see www.iso.org/patents).

Any trade name used in this document is information given for the convenience of users and does not constitute an endorsement.

For an explanation of the voluntary nature of standards, the meaning of ISO specific terms and expressions related to conformity assessment, as well as information about ISO's adherence to the World Trade Organization (WTO) principles in the Technical Barriers to Trade (TBT), see www.iso.org/iso/foreword.html.

This document was prepared by Technical Committee ISO/TC 20, *Aircraft and space vehicles*, Subcommittee SC 14, *Space systems and operations*.

This second edition cancels and replaces the first edition (ISO 14222:2013), which has been technically revised.

The main changes are as follows:

— updated formulae, references to models, indices and links to websites;

— this document now applies to the Earth's atmosphere from ground level upward through the exosphere.

Any feedback or questions on this document should be directed to the user's national standards body. A complete listing of these bodies can be found at www.iso.org/members.html.

Introduction

This document provides guidance for determining the properties of the Earth's atmosphere from ground level upward to the exosphere.

In the atmospheric regions up to approximately 100 km, a detailed knowledge of the average structure of the atmosphere as a function of geographic location, time in the year and solar activity is critical for the design of aircraft, balloon payloads, rocket launch activities and many other facets of modern society. The maximum departures from average conditions also need to be understood in order to provide a margin of safety in design and in operations. These features are included in this document.

A good knowledge of temperature, total density, concentrations of gas constituents, and pressure in the region above about 100 km is important for many space missions exploiting the low-earth orbit (LEO) regime below approximately 2 500 km altitude. In addition to the causes of variation of the atmosphere up to 100 km, geomagnetic processes may seriously affect the structure and dynamics of the thermosphere. Aerodynamic forces on the spacecraft, due to the orbital motion of a satellite through a rarefied gas which itself can have variable high velocity winds, are important for planning satellite lifetime, maintenance of orbits, collision avoidance manoeuvring and debris monitoring, sizing the necessary propulsion system, design of attitude control system, and estimating the peak accelerations and torques imposed on sensitive payloads. Surface corrosion effects due to the impact of large fluxes of atomic oxygen are assessed to predict the degradation of a wide range of sensitive coatings of spacecraft and instruments. The reactions of atomic oxygen around a spacecraft can also lead to intense "vehicle glow".

The structure of Earth's atmosphere and internationally accepted empirical models that specify the details of the atmosphere are included in this document. The annexes and references provide a detailed description the details of those models. The purpose is to create a standard method for specifying Earth's atmosphere properties (density, temperature, wind etc.) at all altitudes from ground level upward, including the low Earth orbit regime now widely-used for space systems and space operations.

The details of those models are included in Annex A.

Annex B provides a detailed description of the electromagnetic radiation and solar and geomagnetic indices.

Space environment (natural and artificial) — Earth's atmosphere from ground level upward

1 Scope

This document specifies the structure and properties of the Earth's atmosphere from ground level upward. It provides internationally accepted empirical models that specify the details of the atmosphere. It also refers to widely-accepted physical models providing insight into the physical and chemical processes driving the response of the atmosphere.

2 Normative references

There are no normative references in this document.

3 Terms and definitions

For the purposes of this document, the following terms and definitions apply.

ISO and IEC maintain terminology databases for use in standardization at the following addresses:

— ISO Online browsing platform: available at https://www.iso.org/obp

— IEC Electropedia: available at https://www.electropedia.org/

3.1
homosphere
region of the atmosphere that is well mixed

Note 1 to entry: The major species proportional concentrations are independent of height and location.

Note 2 to entry: This region extends from 0 km to ~100 km and includes the temperature-defined regions of the *troposphere* (3.2) (surface up to ~6 km to 18 km altitude), the *stratosphere* (3.3) (~6 km to 18 km up to 50 km altitude), the *mesosphere* (3.4) (~50 km up to about 90 km altitude), and the lowest part of the *thermosphere* (3.5) (~90 km to 125 km).

3.2
troposphere
lowest layer of the Earth's atmosphere

Note 1 to entry: It is also where nearly all weather conditions occur.

Note 2 to entry: The troposphere contains approximately 75 % of the atmosphere's mass and 99 % of the total mass of water vapour and aerosols. The average height of the tropopause is 18 km (11 mi; 59 000 ft) in the tropics, 17 km (11 mi; 56 000 ft) in the middle latitudes, and 6 km (3.7 mi; 20 000 ft) in the polar regions in winter. The global average height of the tropopause is 13 km.

Note 3 to entry: The lowest part of the troposphere, where friction with the Earth's surface influences air flow, is called the planetary boundary layer. The boundary layer is typically a few hundred metres to 4 km deep depending on the landform, latitude, season and time of day. The upper boundary of the troposphere is the tropopause, which is the border between the troposphere and *stratosphere* (3.3). The tropopause is an inversion layer, where the air temperature ceases to decrease with height and remains constant through its thickness.

3.3
stratosphere
second major layer of Earth's atmosphere, immediately above the *troposphere* (3.2) and below the *mesosphere* (3.4)

Note 1 to entry: The stratosphere is stratified (layered) in temperature, with warmer layers higher and cooler layers closer to the Earth; this increase of temperature with altitude is a result of the absorption of the Sun's ultraviolet radiation by the ozone layer. This is in contrast to the *troposphere* (3.2), near the Earth's surface, where temperature decreases with altitude. The border between the *troposphere* (3.2) and stratosphere, the tropopause, marks where this temperature inversion begins. Near the equator, the stratosphere starts at as high as 18 km, around 17 km at midlatitudes, and at about 6 km at the poles. Temperatures range from an average of −51 °C near the tropopause to an average of −15 °C near the stratopause [the boundary with the *mesosphere* (3.4)]. Stratospheric temperatures also vary within the stratosphere as the seasons change, reaching particularly low temperatures in the polar night (winter). Winds in the stratosphere can far exceed those in the *troposphere* (3.2), reaching near 60 m/s in the Southern polar vortex.

3.4
mesosphere
layer of the Earth's atmosphere that is directly above the *stratosphere* (3.3) and directly below the *thermosphere* (3.5)

Note 1 to entry: In the mesosphere, temperature decreases as the altitude increases. This characteristic is used to define its limits: it begins at the top of the *stratosphere* (3.3) (sometimes called the stratopause), and ends at the mesopause, which is the coldest part of Earth's atmosphere with temperatures frequently below −143 °C. The exact upper and lower boundaries of the mesosphere vary with latitude and with season (higher in winter and at the tropics, lower in summer and at the poles), but the lower boundary is usually located at heights from 50 km to 65 km above the Earth's surface and the upper boundary (mesopause) is usually around 85 km to 100 km.

Note 2 to entry: The *stratosphere* (3.3) and the mesosphere are collectively referred to as the "middle atmosphere", which spans heights from approximately 10 km to 100 km. The mesopause, at an altitude of 80 km to 90 km, separates the mesosphere from the *thermosphere* (3.5) – the second-outermost layer of the Earth's atmosphere. This is also approximately the same altitude as the turbopause. Below the turbopause, different chemical species are well mixed due to turbulent eddies. Above this level the atmosphere becomes non-uniform; also, above the turbopause, the scale heights of different chemical species differ by their molecular masses.

3.5
thermosphere
region of the atmosphere between the temperature minimum at the mesopause (~90 km) and the altitude where the vertical scale height is approximately equal to the mean free path (400 km to 600 km altitude, depending on solar and geomagnetic activity levels)

Note 1 to entry: At its lower boundary with the *mesosphere* (3.4), the composition is close to that found at ground level. In the upper thermosphere, the composition is usually mainly atomic oxygen.

3.6
exosphere
region of the atmosphere that extends from the top of the *thermosphere* (3.5) outward

3.7
NRLMSIS 2.0
Naval Research Laboratory mass spectrometer, incoherent scatter radar extended model
model that describes the neutral temperature and species densities in Earth's atmosphere from ground level upward, including the *troposphere* (3.2), *stratosphere* (3.3), *mesosphere* (3.4), *thermosphere* (3.5) and *exosphere* (3.6)

Note 1 to entry: It is based on a very large underlying set of supporting data from satellites, rockets, and radars, with extensive temporal and spatial distribution. It has been extensively tested against experimental data by the international scientific community. The model has a flexible mathematical formulation.

Note 2 to entry: It is valid for use from ground level to the *exosphere* (3.6). Two indices are used in this model: $F_{10,7}$ (both the daily solar flux value of the previous day and the 81-day average centred on the input day) and A_p (geomagnetic daily value)

Note 3 to entry: See References [1] and [2].

3.8
Earth GRAM 2016
Earth GLOBAL reference atmosphere models
models which have been produced on behalf of NASA to describe the terrestrial atmosphere from ground level upward for operational purposes

Note 1 to entry: Earth GRAM 2016 is now available as an open-source C++ computer code that can run on a variety of platforms including PCs and UNIX stations. The software provides a model that offers values for atmospheric parameters such as density, temperature, winds, and constituents for any month and at any altitude and location within the Earth's atmosphere. An earlier version, Earth GRAM 2010 is available in FORTRAN.

Note 2 to entry: Earth GRAM 2016 includes the *troposphere* (3.2), *stratosphere* (3.3), *mesosphere* (3.4), *thermosphere* (3.5) and *exosphere* (3.6).

Note 3 to entry: These models now include options for NRLMSIS 2.0, HWM-14 and JB2008.

Note 4 to entry: See https://software.nasa.gov/software/MFS-32780-2.

Note 5 to entry: It is based on a very large underlying set of supporting data from satellites, rockets, and radars, with extensive temporal and spatial distribution. It has been extensively tested against experimental data by the international scientific community. The model has a flexible mathematical formulation.

Note 6 to entry: It is valid for use from ground level to the *exosphere* (3.6). Two indices are used in this model: $F_{10,7}$ (both the daily solar flux value of the previous day and the 81-day average centred on the input day) and A_p (geomagnetic daily value)

Note 7 to entry: See References [3] and [4].

3.9
JB2008
Jacchia-Bowman 2008 model
model that describes the neutral temperature and the total density in Earth's *thermosphere* (3.5) and *exosphere* (3.6)

Note 1 to entry: See https://spacewx.com/jb2008/.

Note 2 to entry: Its new features lead to a better and more accurate model representation of the mean total density compared with previous models, including the NRLMSISE-00 and NRLMSIS 2.0.

Note 3 to entry: It is valid for use from an altitude of 120 km to 2 500 km in the *exosphere* (3.6). Four solar indices and two geomagnetic activity indices are used in this model: $F_{10,7}$ (both tabular value one day earlier and the 81-day average centred on the input time); $S_{10,7}$ (both tabular value one day earlier and the 81-day average centred on the input time); $M_{10,7}$ (both tabular value five days earlier and the 81-day average centred on the input time); $Y_{10,7}$ (both tabular value five days earlier and the 81-day average centred on the input time); a_p (3 h tabular value); and D_{st} (1 h value) (a_p and D_{st} are both used as inputs to create a dT_c temperature change tabular value on the input time).

Note 4 to entry: See References [5] and [6].

3.10
HWM14
horizontal wind model
comprehensive empirical global model of horizontal winds in the atmosphere

Note 1 to entry: Reference values for the a_p index needed as input for the wind model are given in Annex A.

Note 2 to entry: HWM14 does not include a dependence on solar EUV irradiance. Solar cycle effects on thermospheric winds are generally small during the daytime, but can exceed 20 m/s at night.

Note 3 to entry: HWM14 thermospheric winds at high geomagnetic latitudes during geomagnetically quiet periods should be treated cautiously.

Note 4 to entry: See References [7] and [8].

3.11
DTM-2013
drag temperature model 2013
model that describes the neutral temperature and (major and some minor) species densities in the Earth's atmosphere between an altitude of 120 km to approximately 1 500 km

Note 1 to entry: DTM-2013 is based on a large database going back to the early '70s, but it is mainly constructed with high-resolution CHAMP and GRACE accelerometer-inferred data and GOCE thruster-inferred densities.

Note 2 to entry: It is valid from an altitude of 120 km to approximately 1 500 km in the *exosphere* (3.6). Two indices are used in this model: F_{30} solar flux (both daily solar flux of the previous day and the average of the previous 81-days) and K_p (3 h value delayed by 3 h and the average of the last 24 h).

Note 3 to entry: The DTM model codes (DTM-2009 and DTM-2013) are available for download on the SWAMI project website (swami-h2020.eu/).

Note 4 to entry: See References [9] and [10].

3.12
reanalysis model
model that provides access to corrected data sets for any location and any time around the world

EXAMPLE *ERA5* (3.13) and *NCEP/NCAR reanalysis* (3.14).

Note 1 to entry: Reanalysis models provide specific data for locations and periods of interest (e.g. inter-comparison and calibration measurements) and can also be used to provide examples of extrema of atmospheric conditions, contrasting with the long-term averages represented by the empirical models described in 3.7 to 3.11.

3.13
ERA5
latest ECMWF (European Centre for Medium Range Weather Forecasting) meteorological reanalysis project

Note 1 to entry: The first ECMWF reanalysis product, ERA-15[11], generated reanalyses for approximately 15 years, from December 1978 to February 1994. The second product, ERA-40 (originally intended as a 40-year reanalysis) begins in 1957 (the International Geophysical Year) and covers 45 years to 2002. As a precursor to a revised extended reanalysis product to replace ERA-40, ECMWF released ERA-Interim, which covers the period from 1979 to present.

Note 2 to entry: ERA5[11],[12] is a new reanalysis product which has recently been released by ECMWF as part of Copernicus Climate Change Services.

Note 3 to entry: This product has higher spatial (horizontal) resolution (31 km) and covers the period from 1979 to present. Extension back to 1950 is now available.

Note 4 to entry: In addition to reanalysing all the old data, now using a consistent system, the reanalyses also make use of much archived data that was not available to the original analyses. This allows for the correction of many historical hand-drawn maps, where the estimation of features was common in areas of data sparsity. ERA5 also has the ability to create new maps of parameters at specific atmosphere levels that were not commonly used until more recent times.

Note 5 to entry: Accessing the data: The ERA5 data can be downloaded for research use from ECMWF's homepage (see https://apps.ecmwf.int/data-catalogues/era5/?class=ea) and the National Center for Atmospheric Research data archives. Both require registration.

Note 6 to entry: A Python web API can be used to download a subset of parameters for a selected region and time period.

Note 7 to entry: ERA5 is a *reanalysis model* (3.12).

3.14
NCEP/NCAR reanalysis
continually updated globally gridded data set that represents the state of the Earth's atmosphere, incorporating observations and numerical weather prediction (NWP) model output from 1948 to present

Note 1 to entry: It is a joint product from the National Center for Environmental Prediction (NCEP) and the National Center for Atmospheric Research (NCAR).

Note 2 to entry: Accessing the data: The data is available for free download from the NOAA Earth System Research Laboratory[13] and NCEP.[14]-[18] It is distributed in Netcdf and GRIB files, for which a number of tools and libraries exist.

Note 3 to entry: It is available for download through the NCAR CISL Research Data Archive on the NCEP/NCAR Reanalysis main data page[16].

Note 4 to entry: Since then, NCEP-DOE reanalysis 2[17] and the NCEP CFS reanalysis[18] have been released.

Note 5 to entry: The former focuses in fixing existing bugs with the NCEP/NCAR reanalysis system – most notably surface energy and usage of observed precipitation forcing to the land surface, but otherwise uses a similar numerical model and data assimilation system. The latter is based on the NCEP Climate Forecast System[18].

Note 6 to entry: See https://psl.noaa.gov/data/gridded/data.ncep.reanalysis.html.

Note 7 to entry: NCEP/NCAR reanalysis is a *reanalysis model* (3.12).

3.15
SET HASDM density database
database which is used for scientific studies through a SQL database with open community access

Note 1 to entry: The information content of the database originated from the highly accurate densities used to create the NORAD satellite catalogue and produced by the US Air Force through its High Accuracy Satellite Drag Model (HASDM) system.

Note 2 to entry: The historical database covers the period from January 1, 2000 through December 31, 2019. Data records exist every 3 h during solar cycles 23 and 24.

Note 3 to entry: The database has a grid size of 10° × 15° (latitude, longitude) with 25 km altitude steps between 175 km to 825 km.

Note 4 to entry: A description of the source of the database, its validation, its information content and its accessibility are provided by Reference [19].

Note 5 to entry: See https://spacewx.com/hasdm/.

3.16
first principles atmospheric models
models that use the physical inputs in terms of energy and momentum to the formulae describing the behaviour of the atmosphere and as such describe the self-consistent evolution of the whole atmosphere responding to external forcing from the Sun, the oceans, the magnetosphere and solar wind

Note 1 to entry: They include interactions, calculated self-consistently, with the Earth's ionosphere at higher altitudes (upper *mesosphere* (3.4), *thermosphere* (3.5)).

Note 2 to entry: See References [20] to [28].

3.17
WAM
whole atmosphere model
model developed in collaboration with the NOAA Space Weather Prediction and Environmental Modeling Centers (SWPC and EMC) by vertical extension of the operational Global Forecast System (GFS) model over the last decade

Note 1 to entry: The model has demonstrated remarkable performance in simulating climatology and daily variability of the upper atmosphere and ionosphere driven from below. Coupled to ionosphere-electrodynamics models, it not only reproduced dramatic variations of ionospheric plasma drifts and density distribution observed during sudden stratospheric warmings but also demonstrated predictive capability with lead times up to 2 weeks. WAM has reached a level of maturity to be implemented into operations at the National Weather Service (NWS).

Note 2 to entry: Within the same timeframe NWS also plans to substantially upgrade GFS to the Next Generation Global Prediction System (NGGPS). Specific capabilities of NGGPS include in particular a nonhydrostatic dynamical core and the ability to directly simulate important processes such as tropospheric convection at very high resolution globally and without the need for parameterization. This opens an opportunity for development of the Next Generation WAM (NGWAM). Specific requirements for extension of NGGPS into NGWAM will be discussed and capabilities of the new models in application to the upper atmosphere and ionosphere dynamics, simulation and prediction presented.

Note 3 to entry: See References [20]to [23].

3.18
CTIPe
coupled thermosphere ionosphere plasmasphere electrodynamics model
model that consists of four distinct components: a global *thermosphere* (3.5) model; a high-latitude ionosphere model; a mid and low-latitude ionosphere/plasmasphere model; an electrodynamical calculation of the global dynamo electric field, with all four components running concurrently and fully coupled with respect to energy, momentum and continuity

Note 1 to entry: See References [24] to [28].

4 Symbols and abbreviated terms

a_p	the 3 h planetary geomagnetic index given in nT
A_p	the daily planetary geomagnetic index given in nT
CIRA	COSPAR international reference atmosphere
COSPAR	Committee on Space Research
D_{st}	the hourly disturbance storm time ring current index given in nT
F_{10}	the $F_{10,7}$ solar proxy given in units of solar flux, $\times 10^{-22}$ W m^{-2}
F_{30}	the solar energy proxy that is used in the DTM-2013; it corresponds to the solar radio flux emitted by the Sun at 1,000 megaHertz (30 cm wavelength)
M_{10}	the $M_{10,7}$ solar proxy given in units of solar flux, $\times 10^{-22}$ W m^{-2}
S_{10}	the $S_{10,7}$ solar index given in units of solar flux, $\times 10^{-22}$ W m^{-2}
SET	Space Environment Technologies
URSI	International Union of Radio Science
Y_{10}	the $Y_{10,7}$ solar index given in units of solar flux, $\times 10^{-22}$ W m^{-2}

5 General concept and assumptions

5.1 Earth's atmosphere model use

5.1.1 General

NOTE 1 ISO/TR 11225 provides an extensive listing of many empirical and first principles atmospheric models used since before the beginning of the space age up through the modern era.

The NRLMSIS 2.0[1],[2] should be used for calculating both the neutral temperature and the detailed composition of the atmosphere from ground level upward.

The Earth GRAM 2016[3],[4] should be used for calculating the total atmospheric density from ground level upward.

The JB2008 model[5],[6] should be used for calculating the total atmospheric density from 120 km to the exosphere.

The HWM14[7],[8] should be used for horizontal winds from ground level upward.

The DTM-2013[9],[10] should be used for calculating the total atmospheric density above an altitude of 120 km, for example as used in determining satellite drag in low Earth orbit.

For altitudes below 120 km, NRLMSIS 2.0[1],[2], Earth-GRAM 2016[3],[4], ECMWF ERA5[11],[12], NCEP/NCAR reanalysis[13]-[18] or WAM[20]-[23] should be used for calculating the total air density.

The SET HASDM[19] density database should be used as a baseline reference for solar cycles 23 and 24 thermospheric densities with a time cadence of 3 h, an altitude range of 175 km to 825 km in 25 km steps and a latitude/longitude bin size of 10° × 15°.

WAM[20]-[23] should be used primarily for scientific analysis of specific events, from ground level upward.

CTIPe[24]-[28] should be used for investigations of atmospheric and Ionospheric parameters above approximately 100 km, when the response to specific solar and geomagnetic conditions and events is under investigation.

NOTE 2 This usage follows the advice of the CIRA Working Group, sponsored by COSPAR and URSI, following the resolution of the COSPAR Assembly in Montreal in July 2008.

5.1.2 Application guidance

a) The NRLMSIS 2.0 model for species densities should not be mixed with the JB2008, Earth GRAM 2016 or DTM-2013 for total density.

b) For worst-case high solar activity results and analysis periods not exceeding 1 week, high daily short-term values given in Annex A should be used as input for daily activity together with the high long-term values for the 81-day average activity.

c) For analysis periods longer than 1 week the long-term solar activity activities given in Annex A should be used as input for both the daily and the 81-day averaged values.

d) For analysis periods longer than 1 week and conditions specified in Annex A, the daily and 81-day averaged solar activities given in Annex A should be used.

e) Short-term daily high solar activity values should not be used together with low or moderate long-term solar activity values.

NOTE 1 The NRLMSIS 2.0, Earth GRAM 2016, JB2008, and DTM-2013 can only predict large scale and slow variations, on the order of 1 000 km (given by the highest harmonic component) and 3 h.

Spacecraft can often encounter density variations with smaller temporal and spatial scales. This is partly since the spacecraft are in motion (for example, +100 % or −50 % in 30 s) and partly because smaller-scale disturbances certainly do occur during periods of disturbed geomagnetic activity.

NOTE 2 Reference values for the key indices needed as inputs for the atmosphere models are given in Annex A.

NOTE 3 The $F_{10,7}$ 81-day average solar activity can also be estimated by averaging three successive monthly predicted values.

NOTE 4 Information on density model uncertainties can be found in Annex A and in References [1] to [4].

NOTE 5 For high solar activities, the atmosphere models only give realistic results if high short-term values are combined with high 81-day averaged values.

NOTE 6 High D_{st} values can be used corresponding to low, moderate or high solar activities.

5.2 Earth wind model use

The HWM14[7],[8] should be used from ground level upward.

High daily short-term solar activity values should be used as worst-case for the daily activity but the 81-day average activity should not exceed the high long-term value.

NOTE 1 Reference values for the key indices needed as inputs for the wind model are given in Annex A.

NOTE 2 The $F_{10,7}$ 81-day average solar activity can also be estimated by averaging three successive monthly predicted values as given in Annex A.

NOTE 3 The use of the HWM14 model at high geomagnetic latitudes and for disturbed geomagnetic periods necessitates caution in the interpretation of model results.

5.3 Robustness of standard

The Earth's atmosphere models described in this document are intended to be adapted and improved over time as the international scientific community obtains and assesses high quality data on the atmosphere. Therefore, the users of the models described should ensure they utilize the latest version of the respective models.

There are subtle differences between the recommended models.

These reflect differences between the selection of the very many data sources used in these models, although these generally overlap or may even be identical in many cases. However, the weighting applied to the individual data sets may differ. The mathematical formulation of the various empirical models is also distinct.

Differences between the model's predictions for specific location and conditions are generally small compared with the variability of the atmosphere. Users may find that one specific model is more convenient for their specific application than another. Users should, however, be very careful not to mix and merge atmospheric parameters from one model with those from another distinct model.

5.4 Long-term changes of the atmosphere

As the result of increasing levels of CO_2 and CH_4 in the Earth's atmosphere, the mean temperature of the troposphere and stratosphere have warmed, due to the increased thermal blanketing effect. At higher levels – the mesopause and lower thermosphere, the thermal effect is reversed since increased mixing ratios of these thermally-active gases are free to radiate to cold space. The result is a cooling of the upper mesosphere and lower thermosphere and the consequent changes in the thermal and density structure of the middle and upper thermosphere. These effects are highlighted in Figure 1[29].

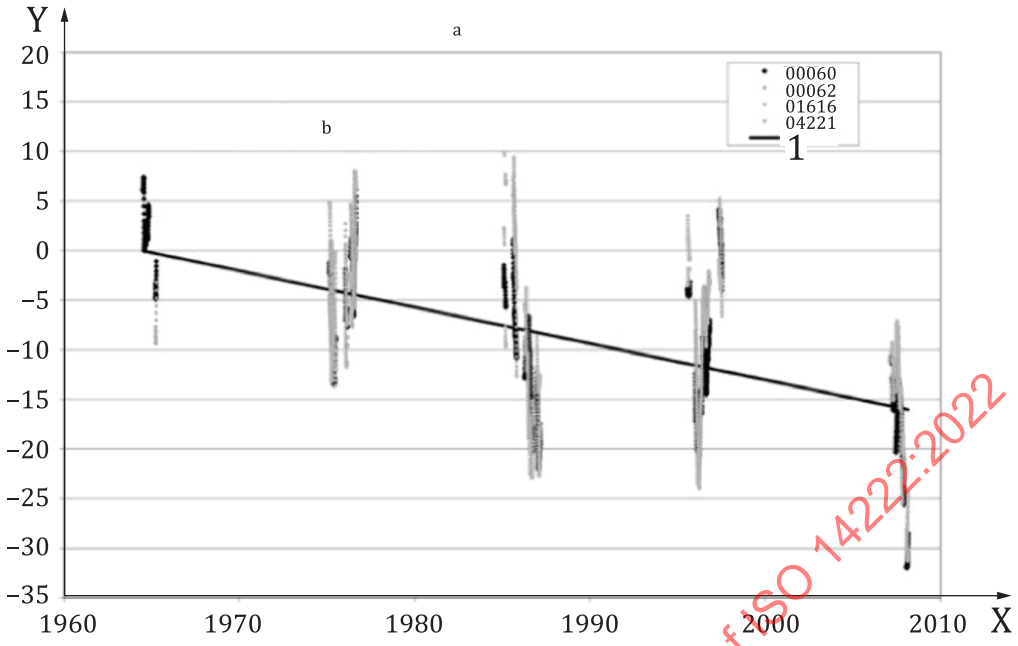

Key

X year

Y dT_c (K)

1 formula

a Change in 81-day exospheric temperature, dT_c, at 400 km for F10B = 68-73.

b Slope = −3,7 degree per decade + −0,1.

= −3,1 % density per decade.

Figure 1 — Changes in temperature at solar minimum at 400 km altitude over 4 solar cycles

These changes of the temperature atmosphere (and consequently density) of the thermosphere are under detailed scrutiny. There are the significant effects on orbital drag (decreased) and the lifetime of artificial satellites and orbital debris (increased). The embedded ionosphere is also affected (for example a reduction in the height of f_0F_2 (height of the maximum of the F_2 region). It is intended that these effects should be analysed in detail and presented in a systematic way in a future revision of this document.

Annex A
(informative)

Neutral atmospheres

A.1 Structure of the Earth's atmosphere

The Earth's atmosphere can be classified into different regions based on temperature, composition, or collision rates among atoms and molecules. For the purposes of the document, the atmosphere is broadly divided into three regimes based on all three properties, as shown in Figure A.1:

a) The homosphere (3.1, 3.2, 3.3, 3.4);

b) The thermosphere (3.5);

c) the exosphere (3.6);

In practice, the boundaries between these regions, whether determined in altitude or in a pressure co-ordinate system, vary with solar, seasonal, latitudinal and other conditions.

Due to winds and turbulent mixing the homosphere has a nearly uniform composition of about 78,1 % N_2, 20,9 % O_2 and 0,9 % Ar. The temperature profile of the thermosphere increases rapidly above a minimum of ~180 K at the mesopause, then gradually relaxes above ~200 km to an asymptotic value known as the exospheric temperature.

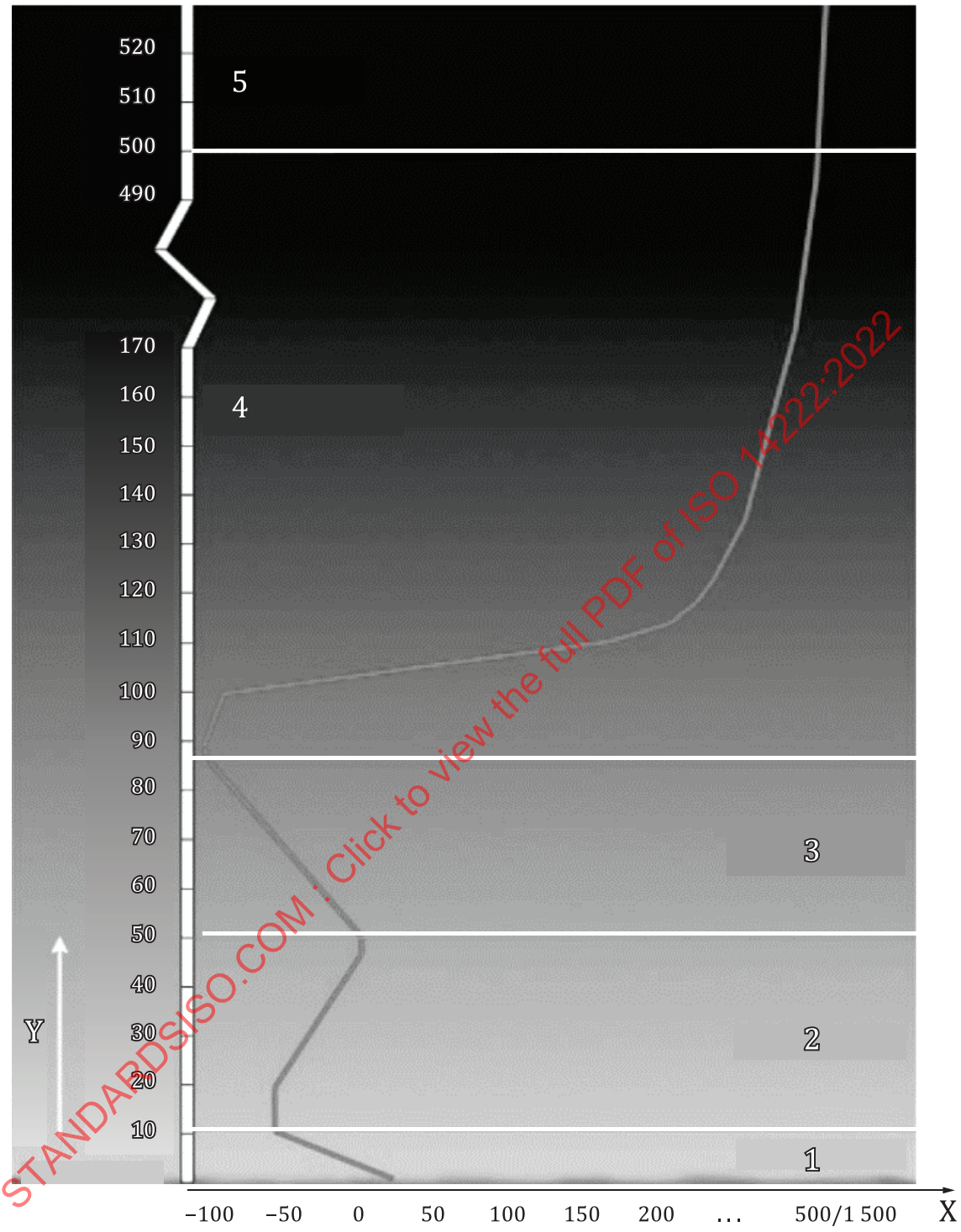

Key

X temperature (Celsius)
Y altitude
1 troposphere
2 stratosphere
3 mesosphere
4 thermosphere
5 exosphere

Figure A.1 — Temperature profile of the Earth's atmosphere

A.2 Development of models of the Earth's atmosphere

A "standard atmosphere" is defined as a vertical distribution of atmospheric temperature, pressure and density, which by international agreement is taken to be representative of the Earth's atmosphere. The first "standard atmospheres" established by international agreement were developed in the 1920's primarily for purposes of pressure altimeter calibrations, aircraft performance calculations, aircraft and rocket design, ballistic tables, etc. Later some countries, notably the United States, also developed and published "standard atmospheres". The term "reference atmosphere" is used to identify vertical descriptions of the atmosphere for specific geographical locations or globally. These were developed by organizations for specific applications, especially as the aerospace industry began to mature after World War II. The term "standard atmosphere" has in recent years also been used by national and international organizations to describe vertical descriptions of atmospheric trace constituents, the ionosphere, atomic oxygen, aerosols, ozone, winds, water vapour, planetary atmospheres, etc.

Currently some of the most commonly used standard and reference atmospheres[30] include: the ISO standard atmosphere 1975, 1982; the U.S. standard atmosphere supplements, 1962, 1966, 1976; the COSPAR international reference atmosphere (CIRA) 1986 (previously issued as CIRA 1961, CIRA 1965 and CIRA 1972); the NASA/MSFC global reference atmosphere model, Earth GRAM 2007 (previously issued as GRAM-86, GRAM-88, GRAM-90, GRAM-95 and GRAM-99); the NRLMSISE-00 thermospheric model 2000 (previously issued as MSIS-77, –83, –86 and MSISE-90); and most recently the JB2006 and JB2008 density models.

A.3 NRLMSIS 2.0 and JB2008 - Additional information

The mass spectrometer and incoherent scatter (MSIS) series of models developed between 1977 and 1990 are used extensively by the scientific community for their superior description of neutral composition. The models utilized atmospheric composition and temperature data from instrumented satellites and ground-based radars. The initial MSIS 1977 model utilized a Bates-Walker temperature profile (which is analytically integrable to obtain density) and allowed the density at 120 km to vary with local time and other geophysical parameters to fit the measurements. The temperature and density parameters describing the vertical profile were expanded in terms of spherical harmonics to represent geographic variations. Subsequent versions of the model include the longitude variations, a refined geomagnetic storm effect, improved high latitude, high solar flux data and an extension of the lower boundary down to sea level.

The NRLMSIS 2.0 model represents atmospheric composition, temperature and total mass density from the ground to the exosphere. Its formulation imposes a physical constraint of hydrostatic equilibrium to produce self-consistent estimates of temperature and density. NRLMSIS 2.0 includes the following enhancements compared to MSISE-90:

a) drag data based on orbit determination;

b) more recent accelerometer data sets;

c) new temperature data derived from Millstone Hill and Arecibo incoherent scatter radar observations;

d) observations of O_2 by the solar maximum mission (SMM), based on solar ultraviolet occultation;

e) a new species, "anomalous oxygen", primarily for drag estimation, allows for appreciable O^+ and hot atomic oxygen contributions to the total mass density at high altitudes.

The Jacchia-Bowman density model (JB2008) is based on the Jacchia model heritage. It includes two key novel features. Firstly, there is a new formulation concerning the semi-annual density variation observed in the thermosphere, but not previously included in any of the semi-empirical atmospheric models. Secondly, there is a new formulation of solar indices, relating more realistically the dependence of heat and energy inputs from the solar radiation to specific altitude regions and heating processes within the upper atmosphere. The D_{st} index (equatorial magnetic perturbation) is used in JB2008 as the index representing the geomagnetic activity response. JB2008 inserts the improved J70 temperature

formulations into the CIRA 1972 model to permit integrating the diffusion equation at every point rather than relying on look-up tables (the integration must be done numerically, in contrast to the analytically integrable Bates-Walker temperature formulation used in MSIS). In order to optimally represent the orbit-derived mass density data on which JB2008 is based, the model formulation sacrifices the physical constraint of hydrostatic equilibrium since it does not include all physical processes that may actually be present in thermosphere affecting temperatures and densities.

A.4 The series of atmosphere models

The National Aeronautics and Space Administration's NASA/MSFC global reference atmospheric model version 2007 (Earth GRAM 2007) is a product of the Natural Environments Branch, NASA Marshall Space Flight Center. These models are available via license to qualified users and provide usability and information quality similar to that of the NRLMSISE-00 model. Like the previous versions of GRAM, the model provides estimates of means and standard deviations for atmospheric parameters such as density, temperature and winds, for any month, at any altitude and location within the Earth's atmosphere. GRAM can also provide profiles of statistically-realistic variations (i.e. with Dryden energy spectral density) for any of these parameters along computed or specified trajectory. This perturbation feature makes GRAM especially useful for Monte-Carlo dispersion analyses of guidance and control systems, thermal protection systems and similar applications. GRAM has found many uses, both inside and outside the NASA community. Most of these applications rely on GRAM's perturbation modelling capability for Monte-Carlo dispersion analyses. Some of these applications have included operational support for shuttle entry, flight simulation software for X-33 and other vehicles, entry trajectory and landing dispersion analyses for the Stardust and Genesis missions, planning for aerocapture and aerobraking for Earth-return from lunar and Mars missions, six-degree-of-freedom entry dispersion analysis for the multiple experiment transporter to Earth orbit and return (METEOR) system and more recently the crew exploration vehicle (CEV). Earth GRAM 2007 retains the capability of the previous version but also contains several new features. The thermosphere has been updated with the new Air Force JB2008 model, while the user still has the option to select the NASA Marshall engineering thermosphere (MET) model or the Naval Research Laboratory (NRL) mass spectrometer, incoherent scatter (MSIS) radar extended model.

A.5 Atmosphere model uncertainties and limitations

For mean activity conditions, the estimated uncertainty of the NRLMSISE-00 species density is 15 %. For short-term and local-scale variations, the estimated uncertainty of the NRLMSISE-00 species density is 100 %. Within the homosphere (below 90 km), the uncertainty is below 5 %. The Earth GRAM 2007 has a similar uncertainty within the homosphere.

For mean activity conditions, the estimated standard uncertainty of the JB2008 total density within the thermosphere is of order 10 % (depending on altitude). For extreme conditions (very high solar or geomagnetic activities), this uncertainty can considerably increase due to the lack of corresponding measurement data. The total density can have ±100 % variation at 400 km to 500 km for some activities and locations.

It should be noted that the models' accuracy of prediction of atmospheric density and other parameters is limited by the complex behaviour of the atmosphere and the causes of variability. While certain aspects of atmospheric variability are more or less deterministic, meteorological variations of the homosphere are difficult to predict more than 3 to 5 days in advance and yet have effects on the thermosphere. In the thermosphere, the response to varying solar and geomagnetic activity is complex, particularly with respect to the latter. Upper atmosphere density models can be used for prediction of future orbital lifetime, either to determine the orbital altitude insertions to ensure a given lifetime, or to estimate energy requirements for maintaining a particular orbit, for a particular spacecraft/satellite. When the sun is active, the primary influence on the accuracy of a model's density output will be the accuracy of the future predictions of solar and geomagnetic activity used as inputs, rather than the accuracy of the specific model in representing the density as a function of solar and geomagnetic activity.

A.6 HWM14 additional information

The HWM series of models empirically represent the horizontal neutral wind in the atmosphere, using a truncated set of vector spherical harmonics. The first edition of the model released in 1987 (HWM87) was intended for winds above 220 km. With the inclusion of wind data from ground-based incoherent scatter radar, MF/meteor radar data and Fabry-Perot optical interferometers, HWM90 was extended down to 100 km. HWM93 extended the model down to the ground. HWM07 is the most recent version of the HWM and includes substantial new space-based data obtained since the early 1990s. Solar cycle variations are included in the earlier models, but they are found to be small and not always very clearly delineated by the current data; HWM07 does not depend on solar activity. HWM07 significantly improves the model's reliability in the lower thermosphere (90 km to 200 km) and under geomagnetically disturbed conditions. However, during quiet conditions, the model does represent polar thermospheric vortices in full detail. The model describes the transition from predominately diurnal variations in the upper thermosphere to semidiurnal variations in the lower thermosphere and a transition from summer to winter flow above 140 km to winter to summer flow below. HWM14 includes substantial further data and improved representation. The model software provides zonal and meridional winds for specified latitude, longitude, altitude, time and 3 h a_p index.

A.7 Reference data

NRLMSIS 2.0 altitude profiles at equatorial latitude of temperature and number densities (concentrations) are listed in Figure A.1, Table A.1 and Table A.2 for low solar and geomagnetic activities ($F_{10,7} = F_{10,7avg} = 65$, $A_p = 0$), moderate solar and geomagnetic activities ($F_{10,7} = F_{10,7avg} = 140$, $A_p = 15$) and high long-term solar and geomagnetic activities ($F_{10,7} = F_{10,7avg} = 250$, $A_p = 45$), respectively. Table A.1 and Table A.2 cover both homospheric and heterospheric altitudes from ground level up to 900 km, averaged over diurnal and seasonal variations.

Figure A.1 illustrates the altitude profile of the temperature.

Figure A.2 shows the atomic oxygen number densities at low, moderate and high long-term activity conditions.

For moderate activity levels, Figure A.3 shows the logarithmic number concentration profiles of the main atmospheric constituents.

Table A.3 provides altitude profiles of the major atmosphere constituents for high long-term solar and geomagnetic activities.

JB2008 short-term, intermediate-term and long-term solar variability reference values are provided in Tables A.4, A.5 and A.6. Figure A.4 shows the variation of the JB2008 mean air density with altitude for low ($F_{10,7} = F_{10,7avg} = 65$, $S_{10,7} = S_{10,7avg} = 60$, $M_{10,7} = M_{10,7avg} = 60$, $Y_{10,7} = Y_{10,7avg} = 60$, $A_p = 0$, $D_{st} = -15$), moderate ($F_{10,7} = F_{10,7avg} = 140$, $S_{10,7} = S_{10,7avg} = 125$, $M_{10,7} = M_{10,7avg} = 125$, $Y_{10,7} = Y_{10,7avg} = 125$, $A_p = 15$, $D_{st} = -15$), high long-term ($F_{10,7} = F_{10,7avg} = 250$, $S_{10,7} = S_{10,7avg} = 220$, $M_{10,7} = M_{10,7avg} = 220$, $Y_{10,7} = Y_{10,7avg} = 220$, $A_p = 45$, $D_{st} = -100$) and high short-term ($F_{10,7} = 300$, $F_{10,7avg} = 250$, $S_{10,7} = 235$, $S_{10,7avg} = 220$, $M_{10,7} = 240$, $M_{10,7avg} = 220$, $Y_{10,7} = Y_{10,7avg} = 220$, $A_p = 240$, $D_{st} = -300$) solar and geomagnetic activity.

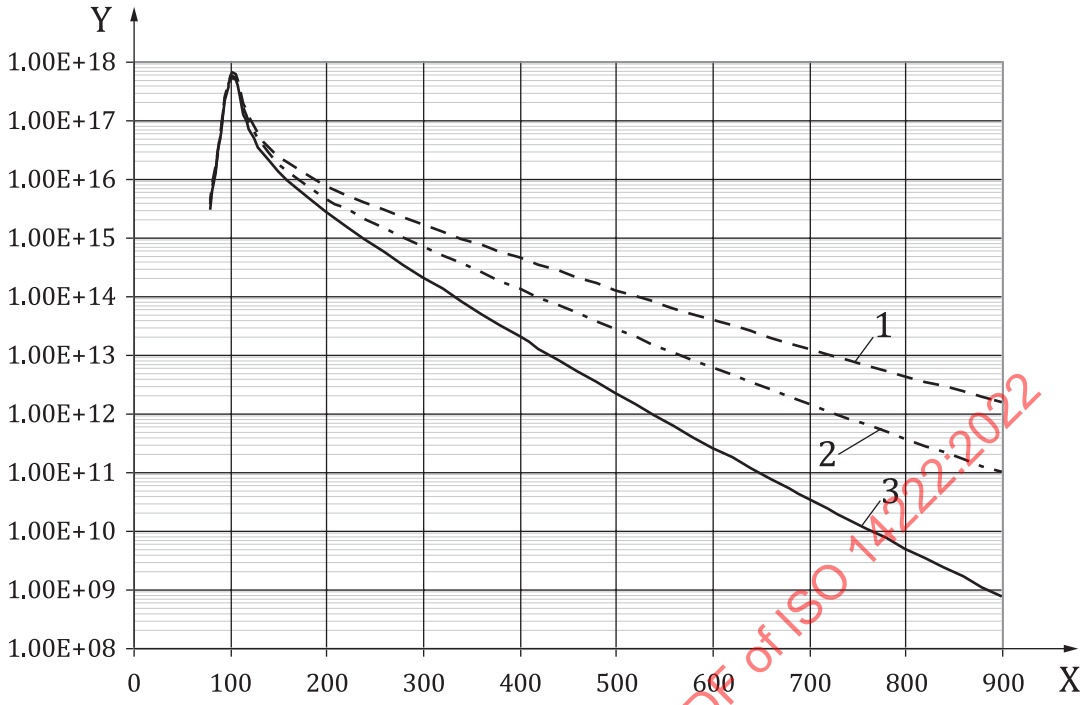

Key

X altitude (km)
Y O density (m^{-3})
1 high activity
2 moderate activity
3 low activity

Figure A.2 — NRLMSIS 2.0 mean atomic oxygen for low, moderate, and high long-term solar and geomagnetic activity

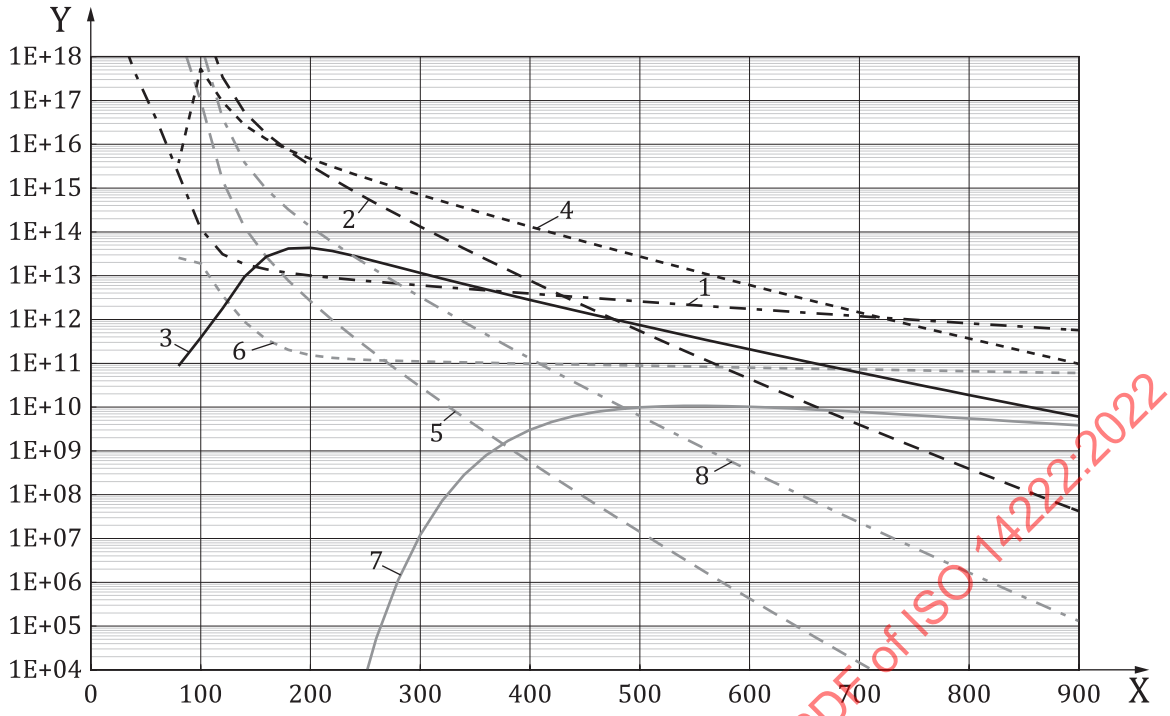

Key

X altitude (km)
1 n_{HE} (/m^3)
2 n_{N2} (/m^3)
3 n_{N} (/m^3)
4 n_{O} (/m^3)
5 n_{AR} (/m^3)
6 n_{H} (/m^3)
7 $n_{Anomal\ O}$ (/m^3)
8 n_{O2} (/m^3)

Figure A.3 — NRLMSIS 2.0 mean concentration of atmosphere constituents for moderate solar and geomagnetic activity

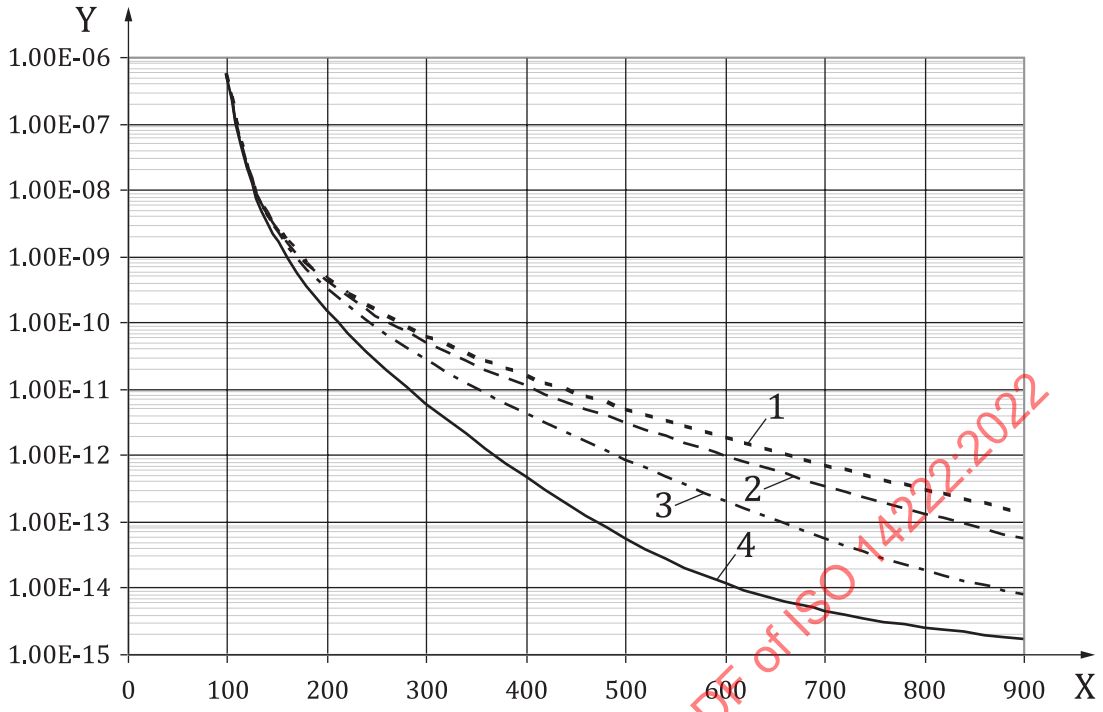

Key

X altitude (km)
Y mass density (kg/m^3)
1 high (shot-term)
2 high (long-term)
3 moderate
4 low

Figure A.4 — JB2008 mean air density with altitude for low, moderate, and high long- and short-term solar and geomagnetic activity

Table A.1 — Altitude profiles of the atmosphere constituents for low solar and geomagnetic activities

H (km)	n_{HE} (m^{-3})	n_O (m^{-3})	n_{N2} (m^{-3})	n_{O2} (m^{-3})	n_{AR} (m^{-3})	n_H (m^{-3})	n_N (m^{-3})	$n_{Anomal\ O}$ (m^{-3})	T(K)	ρ (kg.m^{-3})
0	1.17E+20	0.00E+00	1.74E+25	4.67E+24	2.08E+23	0.00E+00	0.00E+00	0.00E+00	3.00E+02	1.07E+00
20	9.46E+18	0.00E+00	1.41E+24	3.78E+23	1.69E+22	0.00E+00	0.00E+00	0.00E+00	2.06E+02	8.68E-02
40	4.05E+17	0.00E+00	6.04E+22	1.62E+22	7.23E+20	0.00E+00	0.00E+00	0.00E+00	2.57E+02	3.72E-03
60	3.29E+16	0.00E+00	4.90E+21	1.31E+21	5.86E+19	0.00E+00	0.00E+00	0.00E+00	2.45E+02	3.01E-04
80	1.89E+15	3.01E+15	2.73E+20	7.27E+19	3.25E+18	2.65E+13	6.64E+10	2.28E-51	2.06E+02	1.68E-05
100	1.17E+14	4.78E+17	1.02E+19	2.38E+18	1.04E+17	2.70E+13	3.10E+11	2.24E-37	1.71E+02	6.18E-07
120	2.50E+13	7.23E+16	3.11E+17	4.36E+16	1.36E+15	6.07E+12	1.19E+12	1.41E-27	3.53E+02	1.88E-08
140	1.50E+13	2.12E+16	4.89E+16	4.45E+15	1.09E+14	2.17E+12	6.16E+12	2.44E-19	5.21E+02	3.08E-09
160	1.16E+13	9.37E+15	1.38E+16	1.06E+15	1.88E+13	1.09E+12	1.61E+13	1.12E-12	6.05E+02	9.49E-10
180	9.61E+12	4.88E+15	4.76E+15	3.34E+14	4.23E+12	7.31E+11	2.20E+13	1.45E-07	6.48E+02	3.70E-10
200	8.21E+12	2.73E+15	1.80E+15	1.15E+14	1.08E+12	5.94E+11	2.02E+13	1.20E-03	6.70E+02	1.63E-10
220	7.12E+12	1.59E+15	7.14E+14	4.11E+13	2.98E+11	5.32E+11	1.51E+13	1.22E+00	6.82E+02	7.80E-11
240	6.21E+12	9.42E+14	2.93E+14	1.51E+13	8.62E+10	4.98E+11	1.04E+13	2.43E+02	6.88E+02	3.97E-11
260	5.45E+12	5.66E+14	1.23E+14	5.66E+12	2.59E+10	4.75E+11	6.85E+12	1.40E+04	6.92E+02	2.13E-11

Table A.1 *(continued)*

H (km)	n_{HE} (m^{-3})	n_O (m^{-3})	n_{N2} (m^{-3})	n_{O2} (m^{-3})	n_{AR} (m^{-3})	n_H (m^{-3})	n_N (m^{-3})	$n_{Anomal\ O}$ (m^{-3})	T(K)	ρ ($kg.m^{-3}$)
280	4.78E+12	3.44E+14	5.27E+13	2.16E+12	8.02E+09	4.57E+11	4.50E+12	3.08E+05	6.94E+02	1.18E-11
300	4.21E+12	2.10E+14	2.30E+13	8.42E+11	2.54E+09	4.41E+11	2.96E+12	3.26E+06	6.95E+02	6.80E-12
320	3.71E+12	1.30E+14	1.01E+13	3.33E+11	8.22E+08	4.27E+11	1.96E+12	1.96E+07	6.96E+02	4.01E-12
340	3.28E+12	8.05E+13	4.54E+12	1.33E+11	2.71E+08	4.13E+11	1.30E+12	7.64E+07	6.96E+02	2.41E-12
360	2.90E+12	5.02E+13	2.06E+12	5.42E+10	9.06E+07	4.00E+11	8.74E+11	2.13E+08	6.96E+02	1.47E-12
380	2.56E+12	3.15E+13	9.43E+11	2.23E+10	3.07E+07	3.87E+11	5.88E+11	4.60E+08	6.96E+02	9.14E-13
400	2.27E+12	1.99E+13	4.37E+11	9.29E+09	1.06E+07	3.75E+11	3.98E+11	8.15E+08	6.96E+02	5.75E-13
420	2.01E+12	1.26E+13	2.04E+11	3.91E+09	3.66E+06	3.64E+11	2.70E+11	1.24E+09	6.96E+02	3.66E-13
440	1.78E+12	8.06E+12	9.61E+10	1.66E+09	1.29E+06	3.53E+11	1.85E+11	1.69E+09	6.96E+02	2.35E-13
460	1.58E+12	5.17E+12	4.56E+10	7.13E+08	4.55E+05	3.42E+11	1.26E+11	2.09E+09	6.96E+02	1.53E-13
480	1.41E+12	3.33E+12	2.18E+10	3.09E+08	1.63E+05	3.32E+11	8.68E+10	2.42E+09	6.96E+02	1.01E-13
500	1.25E+12	2.15E+12	1.05E+10	1.35E+08	5.87E+04	3.22E+11	5.99E+10	2.66E+09	6.96E+02	6.79E-14
520	1.11E+12	1.40E+12	5.11E+09	5.92E+07	2.13E+04	3.12E+11	4.15E+10	2.81E+09	6.96E+02	4.63E-14
540	9.91E+11	9.14E+11	2.50E+09	2.62E+07	7.81E+03	3.03E+11	2.88E+10	2.88E+09	6.96E+02	3.21E-14
560	8.83E+11	5.99E+11	1.23E+09	1.17E+07	2.88E+03	2.94E+11	2.00E+10	2.88E+09	6.96E+02	2.28E-14
580	7.88E+11	3.94E+11	6.07E+08	5.24E+06	1.07E+03	2.85E+11	1.40E+10	2.83E+09	6.96E+02	1.65E-14
600	7.04E+11	2.60E+11	3.02E+08	2.36E+06	4.01E+02	2.77E+11	9.79E+09	2.74E+09	6.96E+02	1.23E-14
620	6.29E+11	1.73E+11	1.51E+08	1.07E+06	1.51E+02	2.69E+11	6.88E+09	2.63E+09	6.96E+02	9.37E-15
640	5.63E+11	1.15E+11	7.59E+07	4.90E+05	5.74E+01	2.61E+11	4.84E+09	2.50E+09	6.96E+02	7.33E-15
660	5.04E+11	7.67E+10	3.84E+07	2.25E+05	2.19E+01	2.54E+11	3.42E+09	2.37E+09	6.96E+02	5.88E-15
680	4.51E+11	5.14E+10	1.95E+07	1.04E+05	8.42E+00	2.46E+11	2.42E+09	2.23E+09	6.96E+02	4.83E-15
700	4.04E+11	3.45E+10	9.94E+06	4.84E+04	3.26E+00	2.39E+11	1.72E+09	2.09E+09	6.96E+02	4.04E-15
720	3.63E+11	2.33E+10	5.10E+06	2.26E+04	1.27E+00	2.33E+11	1.22E+09	1.96E+09	6.96E+02	3.44E-15
740	3.26E+11	1.58E+10	2.63E+06	1.06E+04	4.97E-01	2.26E+11	8.70E+08	1.83E+09	6.96E+02	2.98E-15
760	2.93E+11	1.07E+10	1.36E+06	5.00E+03	1.96E-01	2.20E+11	6.21E+08	1.70E+09	6.96E+02	2.61E-15
780	2.63E+11	7.28E+09	7.06E+05	2.37E+03	7.75E-02	2.14E+11	4.45E+08	1.59E+09	6.96E+02	2.31E-15
800	2.37E+11	4.97E+09	3.68E+05	1.13E+03	3.09E-02	2.08E+11	3.20E+08	1.48E+09	6.96E+02	2.06E-15
820	2.13E+11	3.40E+09	1.93E+05	5.41E+02	1.24E-02	2.02E+11	2.30E+08	1.38E+09	6.96E+02	1.85E-15
840	1.92E+11	2.33E+09	1.02E+05	2.60E+02	4.99E-03	1.97E+11	1.66E+08	1.28E+09	6.96E+02	1.67E-15
860	1.73E+11	1.61E+09	5.36E+04	1.26E+02	2.02E-03	1.91E+11	1.20E+08	1.19E+09	6.96E+02	1.51E-15
880	1.57E+11	1.11E+09	2.85E+04	6.09E+01	8.25E-04	1.86E+11	8.68E+07	1.11E+09	6.96E+02	1.38E-15
900	1.41E+11	7.67E+08	1.52E+04	2.97E+01	3.38E-04	1.81E+11	6.30E+07	1.03E+09	6.96E+02	1.26E-15

Table A.2 — Altitude profiles of the atmosphere constituents for mean solar and geomagnetic activities

H (km)	n_{HE} (m^{-3})	n_O (m^{-3})	n_{N2} (m^{-3})	n_{O2} (m^{-3})	n_{AR} (m^{-3})	n_H (m^{-3})	n_N (m^{-3})	$n_{Anomal\ O}$ (m^{-3})	T(K)	ρ ($kg.m^{-3}$)
0	1.26E+20	0.00E+00	1.88E+25	5.04E+24	2.25E+23	0.00E+00	0.00E+00	0.00E+00	3.00E+02	1.16E+00
20	1.02E+19	0.00E+00	1.52E+24	4.09E+23	1.82E+22	0.00E+00	0.00E+00	0.00E+00	2.06E+02	9.37E-02
40	4.38E+17	0.00E+00	6.53E+22	1.75E+22	7.81E+20	0.00E+00	0.00E+00	0.00E+00	2.57E+02	4.02E-03
60	3.55E+16	0.00E+00	5.29E+21	1.42E+21	6.33E+19	0.00E+00	0.00E+00	0.00E+00	2.45E+02	3.26E-04
80	2.07E+15	3.71E+15	3.00E+20	7.66E+19	3.56E+18	2.53E+13	8.61E+10	8.53E-51	1.98E+02	1.83E-05
100	1.16E+14	5.22E+17	9.60E+18	2.00E+18	9.71E+16	1.89E+13	3.76E+11	7.28E-37	1.88E+02	5.73E-07
120	3.08E+13	9.27E+16	3.36E+17	3.95E+16	1.49E+15	3.47E+12	1.77E+12	5.52E-27	3.65E+02	2.03E-08
140	1.83E+13	2.73E+16	5.38E+16	3.84E+15	1.26E+14	8.82E+11	9.45E+12	8.98E-19	6.10E+02	3.44E-09

Table A.2 *(continued)*

H (km)	n_{HE} (m^{-3})	n_O (m^{-3})	n_{N2} (m^{-3})	n_{O2} (m^{-3})	n_{AR} (m^{-3})	n_H (m^{-3})	n_N (m^{-3})	$n_{Anomal\ O}$ (m^{-3})	T(K)	ρ ($kg.m^{-3}$)
160	1.39E+13	1.31E+16	1.72E+16	9.29E+14	2.64E+13	3.46E+11	2.73E+13	4.12E-12	7.59E+02	1.20E-09
180	1.16E+13	7.47E+15	7.08E+15	3.22E+14	7.67E+12	2.01E+11	4.18E+13	5.33E-07	8.53E+02	5.46E-10
200	1.00E+13	4.67E+15	3.27E+15	1.31E+14	2.61E+12	1.53E+11	4.31E+13	4.43E-03	9.11E+02	2.84E-10
220	8.91E+12	3.06E+15	1.62E+15	5.81E+13	9.73E+11	1.33E+11	3.64E+13	4.48E+00	9.49E+02	1.61E-10
240	8.00E+12	2.07E+15	8.36E+14	2.71E+13	3.84E+11	1.23E+11	2.82E+13	8.94E+02	9.73E+02	9.60E-11
260	7.24E+12	1.43E+15	4.44E+14	1.31E+13	1.58E+11	1.17E+11	2.10E+13	5.14E+04	9.88E+02	5.97E-11
280	6.59E+12	9.94E+14	2.40E+14	6.48E+12	6.69E+10	1.13E+11	1.56E+13	1.14E+06	9.98E+02	3.83E-11
300	6.01E+12	7.00E+14	1.32E+14	3.27E+12	2.90E+10	1.10E+11	1.15E+13	1.20E+07	1.00E+03	2.52E-11
320	5.50E+12	4.96E+14	7.35E+13	1.67E+12	1.28E+10	1.07E+11	8.60E+12	7.22E+07	1.01E+03	1.69E-11
340	5.04E+12	3.54E+14	4.13E+13	8.66E+11	5.75E+09	1.05E+11	6.45E+12	2.81E+08	1.01E+03	1.16E-11
360	4.62E+12	2.54E+14	2.35E+13	4.54E+11	2.61E+09	1.02E+11	4.86E+12	7.85E+08	1.01E+03	7.99E-12
380	4.24E+12	1.83E+14	1.34E+13	2.40E+11	1.20E+09	1.00E+11	3.68E+12	1.69E+09	1.01E+03	5.60E-12
400	3.90E+12	1.32E+14	7.74E+12	1.28E+11	5.61E+08	9.79E+10	2.79E+12	3.00E+09	1.02E+03	3.96E-12
420	3.59E+12	9.56E+13	4.50E+12	6.90E+10	2.64E+08	9.59E+10	2.13E+12	4.57E+09	1.02E+03	2.83E-12
440	3.30E+12	6.96E+13	2.63E+12	3.74E+10	1.25E+08	9.38E+10	1.63E+12	6.21E+09	1.02E+03	2.03E-12
460	3.04E+12	5.08E+13	1.55E+12	2.05E+10	6.00E+07	9.19E+10	1.25E+12	7.70E+09	1.02E+03	1.47E-12
480	2.80E+12	3.72E+13	9.15E+11	1.13E+10	2.90E+07	9.00E+10	9.59E+11	8.92E+09	1.02E+03	1.07E-12
500	2.58E+12	2.73E+13	5.44E+11	6.24E+09	1.41E+07	8.81E+10	7.39E+11	9.81E+09	1.02E+03	7.85E-13
520	2.38E+12	2.01E+13	3.26E+11	3.48E+09	6.90E+06	8.64E+10	5.71E+11	1.04E+10	1.02E+03	5.78E-13
540	2.20E+12	1.48E+13	1.96E+11	1.95E+09	3.40E+06	8.46E+10	4.42E+11	1.06E+10	1.02E+03	4.29E-13
560	2.03E+12	1.10E+13	1.18E+11	1.10E+09	1.69E+06	8.29E+10	3.43E+11	1.06E+10	1.02E+03	3.19E-13
580	1.88E+12	8.17E+12	7.19E+10	6.24E+08	8.42E+05	8.12E+10	2.67E+11	1.04E+10	1.02E+03	2.39E-13
600	1.74E+12	6.08E+12	4.38E+10	3.55E+08	4.23E+05	7.96E+10	2.08E+11	1.01E+10	1.02E+03	1.80E-13
620	1.61E+12	4.54E+12	2.68E+10	2.04E+08	2.13E+05	7.81E+10	1.62E+11	9.69E+09	1.02E+03	1.36E-13
640	1.49E+12	3.40E+12	1.65E+10	1.17E+08	1.08E+05	7.65E+10	1.27E+11	9.22E+09	1.02E+03	1.04E-13
660	1.38E+12	2.55E+12	1.02E+10	6.78E+07	5.52E+04	7.50E+10	9.91E+10	8.72E+09	1.02E+03	7.98E-14
680	1.28E+12	1.92E+12	6.33E+09	3.94E+07	2.83E+04	7.36E+10	7.78E+10	8.20E+09	1.02E+03	6.16E-14
700	1.18E+12	1.45E+12	3.94E+09	2.30E+07	1.46E+04	7.22E+10	6.11E+10	7.70E+09	1.02E+03	4.80E-14
720	1.10E+12	1.09E+12	2.46E+09	1.34E+07	7.54E+03	7.08E+10	4.81E+10	7.20E+09	1.02E+03	3.76E-14
740	1.02E+12	8.27E+11	1.54E+09	7.91E+06	3.92E+03	6.94E+10	3.80E+10	6.73E+09	1.02E+03	2.98E-14
760	9.45E+11	6.28E+11	9.72E+08	4.67E+06	2.05E+03	6.81E+10	3.00E+10	6.28E+09	1.02E+03	2.38E-14
780	8.78E+11	4.78E+11	6.14E+08	2.77E+06	1.07E+03	6.68E+10	2.37E+10	5.85E+09	1.02E+03	1.92E-14
800	8.16E+11	3.64E+11	3.89E+08	1.65E+06	5.65E+02	6.56E+10	1.88E+10	5.45E+09	1.02E+03	1.57E-14
820	7.58E+11	2.78E+11	2.47E+08	9.83E+05	2.99E+02	6.44E+10	1.49E+10	5.07E+09	1.02E+03	1.29E-14
840	7.05E+11	2.13E+11	1.58E+08	5.89E+05	1.59E+02	6.32E+10	1.19E+10	4.72E+09	1.02E+03	1.07E-14
860	6.56E+11	1.63E+11	1.01E+08	3.54E+05	8.47E+01	6.20E+10	9.45E+09	4.40E+09	1.02E+03	9.03E-15
880	6.11E+11	1.26E+11	6.47E+07	2.14E+05	4.53E+01	6.09E+10	7.54E+09	4.09E+09	1.02E+03	7.67E-15
900	5.69E+11	9.68E+10	4.16E+07	1.29E+05	2.44E+01	5.98E+10	6.02E+09	3.81E+09	1.02E+03	6.59E-15

Table A.3 — Altitude profiles of the atmosphere constituents for high long-term solar and geomagnetic activities

H (km)	n_{HE} (m^{-3})	n_O (m^{-3})	n_{N2} (m^{-3})	n_{O2} (m^{-3})	n_{AR} (m^{-3})	n_H (m^{-3})	n_N (m^{-3})	$n_{Anomal\ O}$ (m^{-3})	T(K)	ρ ($kg.m^{-3}$)
0	1.41E+20	0.00E+00	2.10E+25	5.65E+24	2.52E+23	0.00E+00	0.00E+00	0.00E+00	3.00E+02	1.29E+00
20	1.14E+19	0.00E+00	1.71E+24	4.57E+23	2.04E+22	0.00E+00	0.00E+00	0.00E+00	2.06E+02	1.05E-01

Table A.3 *(continued)*

H (km)	n_{HE} (m^{-3})	n_O (m^{-3})	n_{N2} (m^{-3})	n_{O2} (m^{-3})	n_{AR} (m^{-3})	n_H (m^{-3})	n_N (m^{-3})	$n_{Anomal\ O}$ (m^{-3})	T(K)	ρ ($kg.m^{-3}$)
40	4.90E+17	0.00E+00	7.31E+22	1.96E+22	8.74E+20	0.00E+00	0.00E+00	0.00E+00	2.57E+02	4.49E-03
60	3.98E+16	0.00E+00	5.92E+21	1.59E+21	7.09E+19	0.00E+00	0.00E+00	0.00E+00	2.45E+02	3.64E-4
80	2.34E+15	4.36E+15	3.39E+20	8.15E+19	4.02E+18	2.51E+13	1.23E+11	2.04E-50	1.93E+02	2.03E-05
100	1.21E+14	5.70E+17	9.71E+18	1.72E+18	9.73E+16	1.43E+13	5.38E+11	1.57E-36	2.02E+02	5.64E-07
120	3.61E+13	1.15E+17	3.72E+17	3.37E+16	1.62E+15	2.13E+12	3.08E+12	1.36E-26	3.80E+02	2.22E-08
140	2.09E+13	3.51E+16	6.07E+16	3.02E+15	1.43E+14	3.93E+11	1.76E+13	2.12E-18	7.10E+02	3.93E-09
160	1.59E+13	1.86E+16	2.17E+16	6.80E+14	3.51E+13	1.24E+11	5.84E+13	9.74E-12	9.16E+02	1.54E-09
180	1.34E+13	1.15E+16	1.00E+16	2.29E+14	1.21E+13	6.34E+10	1.02E+14	1.26E-06	1.05E+03	7.87E-10
200	1.17E+13	7.72E+15	5.24E+15	9.68E+13	4.91E+12	4.52E+10	1.18E+14	1.05E-02	1.14E+03	4.57E-10
220	1.05E+13	5.42E+15	2.93E+15	4.65E+13	2.18E+12	3.83E+10	1.09E+14	1.06E+01	1.19E+03	2.86E-10
240	9.62E+12	3.93E+15	1.71E+15	2.42E+13	1.03E+12	3.51E+10	9.18E+13	2.11E+03	1.23E+03	1.87E-10
260	8.85E+12	2.90E+15	1.03E+15	1.32E+13	5.02E+11	3.34E+10	7.39E+13	1.22E+05	1.25E+03	1.27E-10
280	8.19E+12	2.17E+15	6.30E+14	7.43E+12	2.52E+11	3.23E+10	5.87E+13	2.68E+06	1.27E+03	8.87E-11
300	7.60E+12	1.64E+15	3.91E+14	4.28E+12	1.30E+11	3.15E+10	4.65E+13	2.84E+07	1.28E+03	6.31E-11
320	7.07E+12	1.25E+15	2.46E+14	2.51E+12	6.77E+10	3.08E+10	3.70E+13	1.71E+08	1.29E+03	4.56E-11
340	6.59E+12	9.53E+14	1.56E+14	1.49E+12	3.59E+10	3.02E+10	2.95E+13	6.65E+08	1.30E+03	3.34E-11
360	6.16E+12	7.32E+14	1.00E+14	8.94E+11	1.93E+10	2.97E+10	2.36E+13	1.85E+09	1.30E+03	2.47E-11
380	5.75E+12	5.65E+14	6.44E+13	5.41E+11	1.05E+10	2.91E+10	1.90E+13	4.00E+09	1.30E+03	1.85E-11
400	5.38E+12	4.37E+14	4.18E+13	3.30E+11	5.75E+09	2.86E+10	1.54E+13	7.10E+09	1.30E+03	1.40E-11
420	5.04E+12	3.39E+14	2.73E+13	2.03E+11	3.18E+09	2.82E+10	1.24E+13	1.08E+10	1.30E+03	1.06E-11
440	4.72E+12	2.64E+14	1.79E+13	1.26E+11	1.78E+09	2.77E+10	1.01E+13	1.47E+10	1.31E+03	8.13E-12
460	4.42E+12	2.06E+14	1.18E+13	7.84E+10	1.00E+09	2.72E+10	8.21E+12	1.82E+10	1.31E+03	6.26E-12
480	4.14E+12	1.62E+14	7.85E+12	4.91E+10	5.66E+08	2.68E+10	6.69E+12	2.11E+10	1.31E+03	4.84E-12
500	3.89E+12	1.27E+14	5.23E+12	3.10E+10	3.23E+08	2.64E+10	5.47E+12	2.32E+10	1.31E+03	3.76E-12
520	3.65E+12	9.97E+13	3.50E+12	1.96E+10	1.85E+08	2.60E+10	4.48E+12	2.45E+10	1.31E+03	2.94E-12
540	3.43E+12	7.86E+13	2.36E+12	1.25E+10	1.07E+08	2.55E+10	3.67E+12	2.51E+10	1.31E+03	2.31E-12
560	3.22E+12	6.21E+13	1.59E+12	8.01E+09	6.21E+07	2.51E+10	3.02E+12	2.51E+10	1.31E+03	1.82E-12
580	3.02E+12	4.92E+13	1.08E+12	5.15E+09	3.62E+07	2.48E+10	2.48E+12	2.47E+10	1.31E+03	1.43E-12
600	2.84E+12	3.91E+13	7.34E+11	3.33E+09	2.13E+07	2.44E+10	2.04E+12	2.39E+10	1.31E+03	1.14E-12
620	2.67E+12	3.11E+13	5.02E+11	2.16E+09	1.25E+07	2.40E+10	1.69E+12	2.29E+10	1.31E+03	9.06E-13
640	2.52E+12	2.48E+13	3.44E+11	1.41E+09	7.41E+06	2.36E+10	1.39E+12	2.18E+10	1.31E+03	7.23E-13
660	2.37E+12	1.98E+13	2.37E+11	9.19E+08	4.41E+06	2.33E+10	1.15E+12	2.06E+10	1.31E+03	5.79E-13
680	2.23E+12	1.58E+13	1.63E+11	6.03E+08	2.63E+06	2.29E+10	9.57E+11	1.94E+10	1.31E+03	4.65E-13
700	2.10E+12	1.27E+13	1.13E+11	3.97E+08	1.58E+06	2.26E+10	7.94E+11	1.82E+10	1.31E+03	3.75E-13
720	1.98E+12	1.02E+13	7.86E+10	2.63E+08	9.50E+05	2.22E+10	6.60E+11	1.70E+10	1.31E+03	3.03E-13
740	1.87E+12	8.21E+12	5.48E+10	1.74E+08	5.74E+05	2.19E+10	5.50E+11	1.59E+10	1.31E+03	2.46E-13
760	1.76E+12	6.62E+12	3.83E+10	1.16E+08	3.48E+05	2.16E+10	4.58E+11	1.48E+10	1.31E+03	2.00E-13
780	1.66E+12	5.35E+12	2.68E+10	7.74E+07	2.12E+05	2.13E+10	3.82E+11	1.38E+10	1.31E+03	1.63E-13
800	1.57E+12	4.33E+12	1.88E+10	5.19E+07	1.29E+05	2.10E+10	3.20E+11	1.29E+10	1.31E+03	1.34E-13
820	1.48E+12	3.51E+12	1.33E+10	3.48E+07	7.93E+04	2.07E+10	2.67E+11	1.20E+10	1.31E+03	1.10E-13
840	1.40E+12	2.85E+12	9.39E+09	2.35E+07	4.87E+04	2.04E+10	2.24E+11	1.12E+10	1.31E+03	9.06E-14
860	1.32E+12	2.32E+12	6.65E+09	1.59E+07	3.01E+04	2.01E+10	1.88E+11	1.04E+10	1.31E+03	7.50E-14
880	1.25E+12	1.89E+12	4.72E+09	1.07E+07	1.86E+04	1.98E+10	1.58E+11	9.67E+09	1.31E+03	6.23E-14
900	1.18E+12	1.54E+12	3.36E+09	7.30E+06	1.16E+04	1.95E+10	1.33E+11	9.01E+09	1.31E+03	6.00E-14

Table A.4 — Reference values for intermediate- and short-term solar variability

	Case 1: Intermediate-term (81 days)[a]			Case 2: Short-term (27 days high activity)[a]			Case 3: Short-term (27 days low activity)[a]		
Daily	Low	Moderate	High	Low	Moderate	High	Low	Moderate	High
$F_{10,7}$	65	120	225	90	165	280	80	105	145
$S_{10,7}$	60	120	215	105	135	185	85	100	120
$M_{10,7}$	60	115	215	95	135	185	80	95	115
$Y_{10,7}$	50	115	180	110	150	185	90	110	135

NOTE 1 Reference index values are provided for intermediate-term variability that includes more than one solar rotation (> 27 days) but for not more than a half solar cycle (< 6 years). The 81-day smoothed minimum, mean and maximum values rounded to the nearest unit of 5 for solar cycle 23 are used for reference low, moderate and high intermediate-term examples, respectively.

NOTE 2 Daily (short-term) solar variability reference values for less than a solar rotation (27 days) are also provided as rounded numbers to the nearest unit of 5. The period of October 14 to November 9, 2003 in solar cycle 23 is used as a reference period when highly variable activity occurred; these are conditions appropriate to the rise of a solar cycle or large events that occur during the decline of a solar cycle. A second period is provided from January 7 to February 2, 2005 when lower variable activity occurred; these are conditions appropriate approaching or leaving the minimum of a solar cycle. In short-term periods, higher values have been measured than those given, e.g. $F_{10,7}$ = 380 over a day. However, empirical atmosphere density models are not developed for such high index values and their use will lead to large and unknown errors.

[a] The example cases 1, 2 and 3 should use the low, moderate, and high solar activity levels for that case only as one complete set of inputs into JB2008. The 81-day value should be set to the moderate case value for each proxy or index. Values from different case examples should not be mixed. If a single daily value from one case and one solar activity level is desired, the 81-day index should be set to the moderate value for each index.

A.8 JB2008 Long-term solar cycle variability

Tables A.5 and A.6 are provided for estimating solar cycle variability in the four solar indices. The example of solar cycle 23, a moderate cycle, is used. In Tables A.5 and A.6, the actual monthly minimum, mean and maximum value of each index or proxy is given. Table A.5 reports monthly values for the $F_{10,7}$, F_{81} proxy and the $S_{10,7}$, S_{81} index. Table A.6 reports monthly values for the $M_{10,7}$, M_{81} proxy and the $Y_{10.7}$, Y_{81} index.

The ranges of maximum and minimum values are not the confidence values since they are the actual measurements. Smaller solar cycles tend to produce a smaller monthly range; and larger solar cycles tend to produce a larger monthly range. Solar cycle 23 is considered a moderate cycle by recent historical standards.

The tabulated values should be used as provided for periods of up to a solar cycle if no forecasts are available. If daily values are required, the monthly values can be interpolated to daily resolution. Figure A.6 shows all four proxies and indices with their monthly minimum, mean and maximum values. Monthly $F_{10.7}$ forecasts that include confidence bounds are provided by the NOAA SWPC (https://www.swpc.noaa.gov/). Daily forecasts for $F_{10,7}$, F_{81}, $S_{10,7}$, S_{81}, $M_{10,7}$, M_{81}, $Y_{10,7}$ and Y_{81} out to 5 solar rotations (137-days) are provided upon request to Space Environment Technologies (data@spacewx.com).

Table A.5 — Reference values for long-term solar cycle variability in the $F_{10,7}$, F_{81} proxy and $S_{10,7}$, S_{81} index

Month	F_{10min}	F_{10mean}	F_{10max}	F_{81min}	F_{81mean}	F_{81max}	S_{10min}	S_{10mean}	S_{10max}	S_{81min}	S_{81mean}	S_{81max}
0	72	74	77	74	76	78	74	78	82	78	79	79
1	71	74	81	74	74	74	74	77	82	78	78	78
2	70	73	76	74	74	74	73	78	83	78	79	79

Table A.5 *(continued)*

Month	F_{10min}	F_{10mean}	F_{10max}	F_{81min}	F_{81mean}	F_{81max}	S_{10min}	S_{10mean}	S_{10max}	S_{81min}	S_{81mean}	S_{81max}
3	69	74	81	74	74	74	74	80	86	79	80	81
4	71	75	85	72	73	74	78	83	91	81	81	81
5	68	72	77	72	72	73	78	81	87	81	81	82
6	67	71	80	73	74	77	75	80	87	82	83	86
7	71	79	96	78	82	86	80	89	100	86	90	94
8	85	96	119	86	88	91	97	100	103	94	96	99
9	79	85	91	91	92	93	92	98	103	99	100	102
10	86	100	118	93	95	96	97	105	120	102	102	103
11	85	99	117	96	97	97	95	104	114	103	104	105
12	81	93	108	94	95	96	92	104	110	103	104	105
13	83	93	107	95	99	103	93	103	110	104	106	108
14	90	109	133	103	106	108	97	110	123	109	111	113
15	88	108	141	109	110	110	101	117	131	114	115	116
16	87	107	133	106	107	109	103	114	125	116	116	117
17	96	108	122	108	109	111	108	119	128	116	117	117
18	99	114	129	112	119	127	118	118	118	117	118	119
19	109	136	179	127	130	133	118	118	118	118	118	118
20	116	138	177	130	132	133	118	118	118	118	119	122
21	103	117	135	128	130	132	118	120	130	122	125	131
22	115	140	168	132	136	140	123	139	158	131	136	140
23	129	150	184	140	143	147	140	147	159	139	141	142
24	110	141	178	142	145	147	128	136	143	138	139	140
25	99	142	205	135	139	143	115	138	159	137	138	139
26	102	126	156	127	130	135	119	139	154	137	138	139
27	98	117	141	127	130	134	111	132	151	139	141	144
28	127	149	178	134	144	154	130	153	168	145	152	159
29	139	170	210	155	161	167	154	171	192	160	165	170
30	130	166	206	164	166	169	156	172	200	169	170	171
31	123	171	248	155	159	166	146	169	194	161	164	170
32	107	136	163	153	156	159	136	151	184	158	160	162
33	122	165	200	160	165	169	149	159	168	160	162	165
34	143	192	249	169	176	181	157	177	193	165	169	170
35	130	170	217	166	174	178	144	169	192	169	172	173
36	126	158	211	163	167	172	142	167	200	170	171	173
37	138	173	227	172	179	186	155	177	194	174	179	183
38	178	208	234	185	189	192	173	193	213	183	187	189
39	158	184	223	187	191	195	179	192	214	188	189	191
40	127	185	262	181	183	187	165	183	212	184	186	188
41	148	180	202	184	191	196	165	185	206	185	191	195
42	148	202	262	181	185	187	176	207	234	193	196	197

Table A.5 *(continued)*

Month	F_{10min}	F_{10mean}	F_{10max}	F_{81min}	F_{81mean}	F_{81max}	S_{10min}	S_{10mean}	S_{10max}	S_{81min}	S_{81mean}	S_{81max}
43	131	163	194	174	180	184	162	189	213	187	192	195
44	133	182	232	170	171	173	166	181	197	181	183	187
45	140	168	203	173	176	179	166	183	197	181	182	183
46	144	179	205	171	173	176	157	185	224	182	183	184
47	135	174	201	172	174	176	156	184	209	182	183	184
48	152	167	184	160	165	172	172	178	185	175	179	183
49	130	147	170	155	161	167	158	170	184	171	174	176
50	130	178	274	165	168	170	155	175	218	174	174	176
51	123	178	258	169	170	172	152	178	215	173	174	174
52	129	148	185	160	165	171	151	165	186	170	172	174
53	133	174	221	150	153	160	162	176	190	165	167	170
54	115	131	150	151	154	158	142	156	168	166	166	167
55	120	163	199	158	173	187	143	168	180	167	173	181
56	183	234	285	188	203	218	174	199	230	182	191	200
57	171	208	248	218	220	222	192	207	222	201	204	206
58	170	213	271	214	220	226	182	201	232	204	206	209
59	206	236	275	223	224	225	197	211	232	207	209	212
60	189	227	261	217	223	227	197	219	235	211	212	213
61	188	205	246	201	206	216	199	205	218	202	206	211
62	166	179	204	186	193	201	181	191	196	191	196	202
63	147	190	226	181	183	186	171	189	203	183	187	191
64	157	178	191	161	172	181	161	180	194	171	177	183
65	131	149	179	159	162	165	150	163	183	164	166	170
66	129	174	242	163	168	175	144	161	181	163	165	167
67	135	184	241	176	181	183	149	172	202	167	170	172
68	138	176	221	174	178	182	153	174	198	170	172	173
69	136	167	183	164	170	174	150	164	180	163	166	170
70	137	169	199	162	165	169	149	162	176	160	163	166
71	114	157	213	148	157	162	135	164	177	154	158	161
72	115	144	189	136	143	148	133	149	172	144	150	154
73	102	125	150	129	133	136	111	135	151	134	138	143
74	89	132	160	126	127	129	102	131	153	126	130	133
75	99	126	158	121	123	126	109	128	149	123	125	126
76	92	116	149	122	124	126	104	123	142	124	125	126
77	106	129	193	125	126	127	107	125	139	125	126	127
78	99	128	157	122	126	128	108	127	134	125	126	126
79	107	122	137	117	119	122	114	124	136	123	124	125
80	94	112	137	115	122	132	106	121	135	122	123	126
81	92	151	279	129	135	141	110	129	185	123	125	127
82	91	141	210	137	138	140	100	128	153	123	124	126

Table A.5 *(continued)*

Month	F_{10min}	F_{10mean}	F_{10max}	F_{81min}	F_{81mean}	F_{81max}	S_{10min}	S_{10mean}	S_{10max}	S_{81min}	S_{81mean}	S_{81max}
83	86	115	143	121	126	140	92	118	143	117	119	123
84	87	114	135	111	113	120	96	109	126	111	113	117
85	95	107	122	108	110	111	101	109	120	109	111	112
86	90	112	129	105	107	108	101	114	125	109	111	112
87	88	101	117	102	104	105	99	109	117	108	109	110
88	85	100	118	97	99	102	99	104	111	102	105	107
89	82	97	119	97	104	108	93	102	109	102	103	104
90	78	119	175	106	110	112	89	105	125	103	104	105
91	83	110	149	107	112	115	88	105	118	103	105	106
92	88	103	131	102	105	107	93	103	112	102	103	105
93	87	106	140	106	107	108	92	105	122	104	104	105
94	95	114	141	106	106	107	103	108	113	104	104	104
95	85	95	111	99	103	106	92	97	106	99	101	103
96	83	102	145	97	99	100	86	98	119	95	97	98
97	75	97	122	93	97	99	76	94	109	92	94	95
98	74	90	114	90	91	93	76	88	101	88	90	91
99	77	86	106	91	92	93	81	86	92	88	89	90
100	82	100	126	93	95	99	85	92	100	89	90	91
101	77	94	116	94	96	99	82	89	98	90	91	92
102	71	96	130	91	93	95	76	92	107	89	89	90
103	75	91	111	89	91	95	72	88	103	87	88	90
104	72	91	119	85	86	89	74	87	101	84	85	87
105	72	77	83	83	84	85	70	78	83	80	82	84
106	77	86	102	83	85	86	76	80	84	80	81	82
107	85	91	106	86	87	88	79	86	93	82	83	83
108	77	83	94	81	83	86	76	83	89	80	81	83
109	74	77	79	78	79	80	72	76	79	77	78	80
110	72	75	86	79	80	82	71	74	78	77	78	80
111	76	89	101	82	82	83	78	84	92	79	80	82
112	72	81	93	81	82	83	72	83	92	80	81	82
113	72	77	86	76	78	81	73	76	82	76	78	80
114	70	76	87	76	77	78	70	74	82	74	75	76
115	70	79	89	77	78	79	69	73	79	74	74	75
116	70	78	87	78	78	78	67	75	82	74	74	74
117	70	74	80	78	79	81	66	72	78	74	74	75
118	77	86	97	81	83	84	73	77	81	74	74	75
119	72	84	103	84	84	85	68	75	90	75	75	75
120	76	83	92	79	81	84	72	75	80	73	73	74
121	73	78	90	75	77	79	68	72	77	71	72	73
122	69	72	76	73	74	75	64	69	73	68	69	71

Table A.5 *(continued)*

Month	F_{10min}	F_{10mean}	F_{10max}	F_{81min}	F_{81mean}	F_{81max}	S_{10min}	S_{10mean}	S_{10max}	S_{81min}	S_{81mean}	S_{81max}
123	68	72	87	73	73	75	63	67	71	68	68	69
124	67	74	87	74	74	75	66	68	71	68	69	69
125	65	74	87	72	73	75	61	70	79	68	68	69
126	66	72	79	70	71	72	62	67	70	65	66	68
127	67	69	72	68	69	70	62	64	66	63	64	65
128	65	67	71	68	68	68	60	61	65	62	62	63
129	66	68	69	68	68	70	59	62	66	61	61	62
130	67	70	72	70	72	74	59	60	63	61	62	63
131	71	79	94	74	75	75	60	65	71	63	64	65
132	70	74	80	72	74	75	60	67	76	64	64	65
133	70	71	73	72	72	72	61	64	67	63	64	64
134	68	73	89	71	72	72	60	64	72	63	63	63
135	67	70	78	70	71	71	63	66	71	63	63	63
136	66	68	72	67	68	70	60	63	68	62	62	63
137	65	66	67	66	67	67	59	61	63	61	61	62
138	65	66	67	66	66	66	58	61	64	61	61	61
139	65	66	68	66	66	67	59	60	62	60	61	61
140	65	67	69	67	67	68	59	61	63	61	61	61
141	66	68	72	68	68	68	60	63	65	61	62	62
142	67	69	71	69	69	69	60	62	65	61	62	62
143	68	69	71	69	69	69	60	61	63	61	62	62

Table A.6 — Reference values for long-term solar cycle variability in the $M_{10,7}$, M_{81} proxy and $Y_{10,7}$, Y_{81} index

Month	M_{10min}	M_{10mean}	M_{10max}	M_{81min}	M_{81mean}	M_{81max}	Y_{10min}	Y_{10mean}	Y_{10max}	Y_{81min}	Y_{81mean}	Y_{81max}
0	65	72	76	72	73	74	62	66	73	69	71	74
1	62	71	75	72	72	73	63	70	84	69	69	71
2	66	73	80	73	73	74	61	71	80	71	72	72
3	67	75	86	74	75	76	63	74	87	72	73	74
4	72	78	87	76	76	77	64	76	92	72	73	75
5	70	76	86	76	76	77	65	71	86	72	72	73
6	68	75	85	76	77	80	63	70	91	73	75	80
7	73	82	99	80	84	88	65	85	104	81	87	92
8	81	94	101	88	90	92	96	103	110	92	94	98
9	85	91	98	92	93	95	68	90	100	98	100	102
10	84	98	121	95	96	97	98	112	125	101	103	104
11	84	100	120	97	98	99	91	106	120	104	105	106

Table A.6 *(continued)*

Month	M_{10min}	M_{10mean}	M_{10max}	M_{81min}	M_{81mean}	M_{81max}	Y_{10min}	Y_{10mean}	Y_{10max}	Y_{81min}	Y_{81mean}	Y_{81max}
12	85	99	114	97	98	99	77	101	114	102	103	104
13	85	96	107	98	99	102	91	102	116	103	106	111
14	83	103	117	103	106	109	102	115	131	111	114	118
15	94	113	147	109	111	112	105	120	136	118	120	121
16	90	110	129	112	113	114	107	122	138	120	121	122
17	99	115	139	115	117	119	113	122	129	122	123	125
18	111	128	150	119	125	130	117	127	137	125	130	134
19	122	135	148	130	132	134	132	142	162	135	136	138
20	121	137	151	132	134	135	130	140	154	138	139	139
21	109	126	137	131	133	135	123	132	138	138	139	141
22	116	137	169	134	136	138	129	148	162	141	143	145
23	126	146	175	137	139	140	142	149	158	145	148	149
24	109	138	166	137	138	140	126	149	171	146	147	148
25	102	134	172	134	135	138	123	144	167	142	144	147
26	109	130	159	130	132	134	117	136	157	137	138	142
27	97	121	157	131	132	135	115	131	143	137	139	141
28	117	145	175	135	142	150	140	151	172	141	147	152
29	135	163	197	151	156	160	152	159	175	153	156	159
30	132	162	191	159	160	162	140	159	177	158	159	160
31	129	162	202	152	155	161	140	162	181	155	157	159
32	121	142	175	150	152	154	135	147	164	154	155	156
33	131	153	167	153	156	158	144	157	165	156	158	160
34	141	170	195	158	161	164	151	170	184	160	162	163
35	125	159	191	162	165	167	140	158	173	158	161	163
36	129	162	209	163	164	166	138	156	175	157	158	160
37	131	167	193	166	170	174	148	162	174	160	163	166
38	156	185	213	174	178	181	163	173	182	165	166	167
39	164	186	213	178	180	183	153	163	178	165	167	168
40	141	172	210	173	176	179	139	163	188	163	164	165
41	145	174	197	174	181	184	152	164	174	164	168	171
42	156	196	236	181	185	187	152	177	194	167	168	169
43	131	177	220	177	182	183	144	161	176	164	166	168
44	150	173	196	173	174	176	150	164	178	163	163	164
45	153	175	200	173	174	176	153	165	175	164	166	168
46	137	179	211	173	174	176	149	170	183	166	166	167
47	126	174	203	172	174	176	149	164	181	164	165	167
48	148	172	188	165	170	176	154	161	167	156	159	163
49	127	156	179	159	162	165	137	148	162	155	157	160
50	137	158	216	157	159	164	140	166	204	159	160	161
51	116	163	204	158	159	162	144	163	203	161	161	162

Table A.6 *(continued)*

Month	M_{10min}	M_{10mean}	M_{10max}	M_{81min}	M_{81mean}	M_{81max}	Y_{10min}	Y_{10mean}	Y_{10max}	Y_{81min}	Y_{81mean}	Y_{81max}
52	125	154	173	161	161	163	137	150	167	156	158	161
53	147	171	194	159	161	163	147	162	175	152	153	155
54	133	152	172	159	160	161	133	145	153	153	154	157
55	133	157	182	161	166	173	135	160	177	157	162	167
56	172	194	223	173	184	194	167	181	191	167	172	177
57	176	202	234	194	198	201	162	173	182	175	176	177
58	168	192	207	200	202	206	164	175	191	175	176	179
59	196	212	232	203	207	212	171	182	203	179	179	180
60	195	219	243	211	213	214	173	181	188	179	180	180
61	192	207	230	202	206	211	171	177	185	177	177	179
62	176	188	202	190	195	202	166	174	186	176	177	178
63	167	188	212	185	187	190	166	179	190	176	176	177
64	157	184	210	173	180	185	167	175	182	168	172	176
65	143	167	190	166	169	172	153	161	175	167	167	167
66	139	164	201	165	167	169	150	169	188	166	168	170
67	134	174	214	169	173	175	156	175	195	170	171	172
68	144	177	207	174	175	176	151	166	177	168	170	171
69	145	168	190	165	170	173	152	166	180	164	166	168
70	140	163	185	161	165	169	152	166	181	163	165	167
71	130	164	193	153	159	163	135	162	182	155	160	163
72	128	149	182	143	149	154	137	151	167	146	151	155
73	109	130	163	132	137	142	116	138	152	138	142	145
74	94	131	172	126	129	132	113	137	154	135	136	138
75	106	130	158	123	125	126	114	136	161	132	133	134
76	94	122	147	124	125	128	105	130	145	133	134	136
77	103	126	151	127	128	131	122	138	163	135	136	137
78	113	134	150	129	130	131	122	138	152	135	137	137
79	118	129	141	126	128	130	131	135	146	132	134	135
80	106	123	145	125	127	130	118	130	142	131	134	138
81	102	133	187	126	129	133	110	144	185	136	138	141
82	92	134	175	128	129	131	113	142	177	138	139	140
83	84	121	159	121	123	128	100	129	151	128	132	138
84	88	112	152	112	115	120	101	123	143	122	124	128
85	91	108	127	109	111	112	106	117	123	118	120	121
86	90	110	126	107	109	110	108	120	130	115	117	118
87	95	108	122	107	108	109	100	113	135	113	115	116
88	95	104	113	101	104	107	101	111	122	109	111	113
89	87	101	116	101	103	105	94	110	123	109	112	114
90	79	106	142	102	105	106	90	118	143	113	116	118
91	83	106	135	105	107	108	96	119	146	117	120	121

Table A.6 *(continued)*

Month	M_{10min}	M_{10mean}	M_{10max}	M_{81min}	M_{81mean}	M_{81max}	Y_{10min}	Y_{10mean}	Y_{10max}	Y_{81min}	Y_{81mean}	Y_{81max}
92	85	105	131	103	106	108	96	117	136	114	115	117
93	94	108	131	106	107	109	94	111	131	113	115	116
94	99	112	129	107	107	108	107	121	130	113	114	116
95	87	102	116	101	104	107	100	110	122	111	113	115
96	83	98	117	97	99	101	90	110	134	105	108	111
97	74	96	121	94	96	97	76	101	117	100	103	105
98	72	90	113	91	92	94	77	96	118	97	98	99
99	75	88	101	91	92	94	82	95	109	98	100	101
100	92	98	109	93	94	96	93	109	124	101	104	107
101	79	93	107	94	95	97	87	104	116	105	106	108
102	71	95	123	92	93	95	75	106	126	101	103	105
103	72	94	118	90	92	94	79	99	121	97	101	104
104	72	90	105	87	89	91	74	99	115	90	93	98
105	71	81	93	85	86	88	60	77	89	86	88	90
106	76	84	91	84	85	87	81	90	104	86	87	89
107	80	92	107	86	87	87	90	97	108	86	89	91
108	75	86	102	82	85	86	62	82	98	76	81	86
109	72	78	86	79	80	82	53	66	77	72	74	76
110	70	76	81	80	81	83	62	72	88	74	77	82
111	77	88	108	83	84	86	82	91	104	82	84	87
112	69	87	106	84	85	86	74	87	101	85	86	87
113	72	79	87	80	81	84	68	81	91	80	82	86
114	70	79	91	78	78	80	59	78	95	80	80	81
115	67	77	83	77	78	79	63	82	97	79	81	82
116	66	77	92	75	76	78	66	80	93	77	78	80
117	63	72	83	74	75	76	58	69	84	78	78	79
118	63	77	86	74	75	76	72	87	97	79	81	83
119	62	76	89	76	77	77	61	83	106	80	83	84
120	67	77	88	74	75	76	69	81	90	72	76	80
121	67	74	84	71	73	74	56	64	86	66	69	72
122	64	68	74	69	69	71	59	63	70	62	64	66
123	62	68	80	69	69	71	55	65	89	65	66	68
124	64	70	80	70	71	72	57	69	83	68	69	70
125	62	73	89	71	71	72	55	69	87	65	67	70
126	61	70	76	68	69	71	56	64	81	61	63	65
127	60	66	70	66	67	68	56	59	64	58	59	61
128	60	64	67	65	65	66	54	57	61	56	57	58
129	61	64	67	65	65	67	52	55	58	56	56	57
130	62	65	70	68	70	72	55	57	60	58	60	60
131	63	80	94	72	72	72	54	66	86	58	59	60

Table A.6 *(continued)*

Month	M_{10min}	M_{10mean}	M_{10max}	M_{81min}	M_{81mean}	M_{81max}	Y_{10min}	Y_{10mean}	Y_{10max}	Y_{81min}	Y_{81mean}	Y_{81max}
132	61	67	77	68	71	72	46	52	61	52	56	58
133	64	68	74	66	67	67	49	51	55	51	52	53
134	64	67	71	66	67	67	49	55	72	52	53	53
135	62	66	71	66	66	66	47	51	66	52	52	52
136	63	65	70	65	65	66	48	50	53	49	50	52
137	62	63	65	63	64	64	47	48	50	48	49	49
138	60	62	65	62	63	63	46	48	49	48	48	48
139	61	62	63	62	62	62	47	47	48	47	47	48
140	60	62	63	62	62	62	46	47	48	47	47	48
141	61	63	65	62	62	62	47	48	49	48	48	48
142	60	62	65	62	62	62	46	48	49	47	47	48
143	60	61	64	62	62	62	46	47	49	47	47	47

A.9 JB2008 long-term 25-year solar variability

As a guide for orbit lifetime planning and debris mitigation purposes, it is often useful to have a 25-year estimate of atmosphere density variability that is driven by solar indices. The following procedure is recommended for producing a consistent, repeatable estimate of long-term 25-year JB2008 thermospheric densities:

a) Determine the relative starting point in the solar cycle for the proxies and indices from Tables A.5 and A.6; the most useful index for this is the F_{81} mean value in Table A.5; the start may be at the beginning, rise, maximum, decline, or end of a cycle; for example, to plan a mission with a spacecraft launch in 2012 and to estimate its 25-year lifetime, the assumption would be made that the mission start is approximately at the maximum of cycle 24; an appropriate date in cycle 23 would be selected such as month 60 where the F_{81} mean value is 223; the F_{81} mean value can be used a generalized indicator of solar cycle phases.

b) Form a consecutive set of monthly proxy and index values by concatenating onto Tables A.5 and A.6 the month 0 line of the tables starting in place of month 124; although solar cycles are often thought of as 11-year cycles, there is actually a range of cycle periods; and this method results in an acceptable solar cycle length of 124 months (10 years, 4 months) where the discontinuity between the end of one cycle and the start of another cycle is minimized; the cycle start in the table data set is month 0, the peak is month 60 and the cycle end is month 123 when the table is used to create multiple cycles; it is typical for a solar cycle to have a faster rise to maximum and a slower decline to minimum; the solar cycle minimum is the lowest average value following the peak of the cycle; this method has a slight high flux bias by excluding the lowest solar activity conditions and favours shorter solar cycles.

c) Repeat this process for as many months, years, or solar cycles as are needed.

A.10 JB2008 altitude profiles of total density

Table A.7 shows the JB2008 altitude profiles of total density ρ [kg m^{-3}] for low ($F_{10,7} = F_{10,7avg} = 65$, $S_{10,7} = S_{10,7avg} = 60$, $M_{10,7} = M_{10,7avg} = 60$, $Y_{10,7} = Y_{10,7avg} = 60$, $A_p = 0$, $D_{st} = -15$), moderate ($F_{10,7} = F_{10,7avg} = 140$, $S_{10,7} = S_{10,7avg} = 125$, $M_{10,7} = M_{10,7avg} = 125$, $Y_{10,7} = Y_{10,7avg} = 125$, $A_p = 15$, $D_{st} = -15$), high long-term ($F_{10,7} = F_{10,7avg} = 250$, $S_{10,7} = S_{10,7avg} = 220$, $M_{10,7} = M_{10,7avg} = 220$, $Y_{10,7} = Y_{10,7avg} = 220$,

A_p = 45, D_{st} = −100) and high short-term ($F_{10,7}$ = *300*, $F_{10,7avg}$ = 250, $S_{10,7}$ = *235*, $S_{10,7avg}$ = 220, $M_{10,7}$ = *240*, $M_{10,7avg}$ = 220, $Y_{10,7}$ = $Y_{10,7avg}$ = 220, A_p = 240, D_{st} = −300) solar and geomagnetic activity.

Table A.7 — Altitude profiles of total density for low, moderate and high long-and short-term solar and geomagnetic activity

H (km)	Low activity	Moderate activity	High activity (long-term)	High activity (short-term)
100	5.31E-07	5.47E-07	5.44E-07	5.43E-07
120	2.18E-08	2.40E-08	2.45E-08	2.46E-08
140	3.12E-09	3.98E-09	4.32E-09	4.45E-09
160	9.17E-10	1.36E-09	1.54E-09	1.60E-09
180	3.45E-10	6.15E-10	7.40E-10	7.77E-10
200	1.47E-10	3.17E-10	4.10E-10	4.38E-10
220	6.96E-11	1.77E-10	2.46E-10	2.70E-10
240	3.54E-11	1.05E-10	1.56E-10	1.77E-10
260	1.88E-11	6.47E-11	1.04E-10	1.21E-10
280	1.03E-11	4.12E-11	7.12E-11	8.57E-11
300	5.86E-12	2.69E-11	5.00E-11	6.22E-11
320	3.40E-12	1.80E-11	3.59E-11	4.60E-11
340	2.02E-12	1.23E-11	2.61E-11	3.45E-11
360	1.22E-12	8.48E-12	1.93E-11	2.63E-11
380	7.46E-13	5.95E-12	1.44E-11	2.02E-11
400	4.63E-13	4.22E-12	1.09E-11	1.57E-11
420	2.92E-13	3.02E-12	8.32E-12	1.23E-11
440	1.87E-13	2.18E-12	6.40E-12	9.69E-12
460	1.21E-13	1.59E-12	4.96E-12	7.70E-12
480	8.04E-14	1.17E-12	3.87E-12	6.16E-12
500	5.44E-14	8.60E-13	3.04E-12	4.95E-12
520	3.77E-14	6.39E-13	2.40E-12	4.01E-12
540	2.68E-14	4.77E-13	1.91E-12	3.25E-12
560	1.96E-14	3.58E-13	1.52E-12	2.66E-12
580	1.47E-14	2.71E-13	1.22E-12	2.18E-12
600	1.14E-14	2.06E-13	9.82E-13	1.79E-12
620	9.10E-15	1.57E-13	7.93E-13	1.48E-12
640	7.41E-15	1.20E-13	6.43E-13	1.23E-12
660	6.16E-15	9.28E-14	5.22E-13	1.02E-12
680	5.22E-15	7.19E-14	4.25E-13	8.49E-13
700	4.50E-15	5.60E-14	3.47E-13	7.09E-13
720	3.93E-15	4.40E-14	2.84E-13	5.94E-13
740	3.48E-15	3.48E-14	2.34E-13	4.98E-13
760	3.10E-15	2.79E-14	1.92E-13	4.19E-13
780	2.79E-15	2.26E-14	1.59E-13	3.54E-13
800	2.53E-15	1.85E-14	1.32E-13	2.99E-13
820	2.30E-15	1.53E-14	1.10E-13	2.54E-13
840	2.11E-15	1.28E-14	9.21E-14	2.16E-13
860	1.94E-15	1.08E-14	7.72E-14	1.84E-13
880	1.78E-15	9.27E-15	6.50E-14	1.57E-13

Table A.7 *(continued)*

H **(km)**	**Low activity**	**Moderate activity**	**High activity (long-term)**	**High activity (short-term)**
900	1.65E-15	8.01E-15	5.49E-14	1.35E-13

Annex B
(informative)

Natural electromagnetic radiation and indices

B.1 General

A spacecraft in low Earth orbit (LEO) receives electromagnetic radiation from three primary external sources[3]. The largest source is the direct solar flux. The mean value of this solar flux at the mean Earth-Sun distance is called the “solar constant”. It is not really a constant but varies by about 3,4 % during each year because of the slightly elliptical orbit of the Earth about the Sun. The two others radiation sources are the fraction of the incident sunlight reflected off the planet, termed albedo and the Earth's infrared radiation.

Solar and geomagnetic activities are often described by indices. The UV radiation of the Sun, which strongly affects the Earth's atmosphere, cannot be directly measured from the ground. It was, however, found to be strongly correlated with e.g. the sunspot number and the cm wavelength Sun radiation. For example, the widely used 10,7 cm radio flux index ($F_{10,7}$) gives an indication of the solar UV radiation output which is highly variable over a solar cycle.

Geomagnetic indices typically describe the variation of the geomagnetic field over a certain time period. They provide a measure of the disturbance of the magnetosphere which has direct consequences for the charged particle space environment, or the external component of the geomagnetic field.

Solar and geomagnetic indices are used as input for upper atmosphere and other models of the near-Earth space environment. They are provided for short durations or as long-time averages. Predictions for future index values are usually provided at different confidence levels and they are available for complete solar cycles. See A.8. The given data are mainly average values. For detailed thermal analyses or certain special applications, more detailed data and models are required. These are outside the scope of this document.

B.2 Electromagnetic radiation and indices

B.2.1 Solar constant

The solar constant is defined as the radiation that falls on a unit area of surface normal to the line from the Sun, per unit time, outside the atmosphere, at one astronomical unit (1 AU = average Earth-Sun distance). The currently measured 1-sigma standard deviation in the composite dataset is approximately 0,6 Wm^{-2} and there is a long-term (yearly) smoothed solar cycle minimum to maximum relative variation about the mean value of approximately 1,4 Wm^{-2} (largest during the period of maximum solar activity).

B.2.2 Solar spectrum

B.2.2.1 Soft X-rays or XUV (0,1 nm to 10 nm)

Usually associated with solar coronal phenomena, flares, million-degree temperatures, and atomic dissociation, the corona extends from about 21 000 km to about 1 400 000 km above the photosphere. X-ray flares are responsible for enhancements in the D and E regions of the Earth's ionosphere.

B.2.2.2 Extreme ultraviolet or EUV (10 nm to 121 nm)

EUV has emission lines that come from the upper chromosphere (near-coronal temperatures), transition region and lower corona of the Sun. This spectral band is responsible for ionization and heating in the E and F regions of the ionosphere.

B.2.2.3 Ultraviolet or UV (100 nm to 400 nm)

UV solar flux is emitted primarily from the base of the Sun's chromosphere layer and has components due to active and quiet solar conditions. This band is responsible for only 1 % of the total solar irradiance, but it is important because below 300 nm, it is completely absorbed by ozone and diatomic oxygen atoms in the Earth's upper atmosphere.

B.2.2.4 Visible, optical or VIS (380 nm to 760 nm)

Visible light comes from the solar photosphere, which is only about 400 km thick, has a temperature of approximately 5 000 K to 6 000 K and yet is responsible for the greatest percentage of the total solar radiation.

B.2.2.5 Infrared or IR (0,70 µm to 1 mm)

Solar infrared in this range is responsible for the direct heating of the Earth's lower atmosphere, through absorption by H_2O and has an effect on minor species constituents in the Earth's mesosphere and thermosphere.

ISO 21348 on determining solar irradiances provides more details about the solar spectrum.

B.2.3 Solar and geomagnetic indices – additional information

B.2.3.1 General

Solar and geomagnetic indices are used to describe the activity levels of the Sun and the disturbance of the geomagnetic field. Most activity indices are given for short periods and as long duration averages. They are also used for long range predictions of solar activities. Many space environment models require activity index values as input parameters. Geomagnetic activity indices are used to describe fluctuations of the geomagnetic field.

B.2.3.2 Sunspot number (R)

The sunspot number (R, alternatively called R_i or R_z) is a daily index of sunspot activity, defined as

$$R = k(10g + s) \tag{B.1}$$

where

s is the number of individual spots;

g the number of sunspot groups;

k is an observatory factor.

R_{12} (R_{z12}) is the 12-month running mean of the sunspot number R.

B.2.3.3 $F_{10,7}$

$F_{10,7}$ (abbreviated F_{10}) is the traditional solar energy proxy that is used both for NRLMSISE-00 and JB2008 atmosphere models and the Earth GRAM 2007 model. It corresponds to the solar radio flux emitted by the Sun at 2 800 megaHertz (10,7 cm wavelength). The Sun emits radio energy with a

slowly varying intensity. This radio flux, which originates from atmospheric layers high in the Sun's chromosphere and low in its corona, changes gradually from day-to-day in response to the number of spot groups on the disk. Solar flux density at 10,7 cm wavelength has been recorded routinely by radio telescope near Ottawa since February 14, 1947.

Each day, levels are determined at local noon (1700 GMT). Beginning in June 1991, the solar flux density measurement source is Penticton, B.C., Canada. Its observations are available through the Dominion Radio Astrophysical Observatory (DRAO) website and all values are also archived at the Space Physics Interactive Data Resource (SPIDR).

Three sets of fluxes, the observed, the adjusted, and the absolute, are summarized. Of the three, the observed numbers are the least refined, since they contain fluctuations as large as 7 % that arise from the changing Earth-Sun distance. In contrast, adjusted fluxes have this variation removed; the numbers in these tables equal the energy flux received by a detector located at the mean distance between Earth and Sun. Finally, the absolute levels carry the error reduction one step further; here each adjusted value is multiplied by 0,90 to compensate for uncertainties in antenna gain and in waves reflected from the ground.

NOTE The physical units of $F_{10,7}$ are 10^{-22} $Wm^{-2}Hz^{-1}$; the numerical value is used without the multiplier as is customarily done and expressed as solar flux units (sfu). In other words, a 10,7 cm radio emission of 150×10^{-22} W $m^{-2}Hz^{-1}$ is simply referred to as $F_{10,7}$ = 150 sfu.

$F_{10,7}$ and the sunspot number, R, are correlated. Averaged (over one month or longer) values can be converted by Formula (B.2):

$$F_{10,7} = 63,7 + 0,728R + 8,9\times10^{-4} R^2 \quad \text{(B.2)}$$

This correlation was introduced in IRI for the relationship between the 12-month running mean of $F_{10,7}$ and the 12-month running mean of sunspot number. The correlation deteriorates when going to monthly values and the correlation parameters are different. However, the real problem is that this relationship is for the 'old' sunspot number, the revised sunspot number and only one now being generated and distributed by the Belgian centre (https://www.sidc.be/silso/), is a factor of ~0,7 smaller.

B.2.3.4 $E_{10,7}$

Although not used in atmosphere models described earlier, $E_{10,7}$ is the integration in the range from 1 nm to 105 nm of the energy flux of solar irradiance, reported in solar flux units (sfu) or $\times10^{-22}$ Watts per meter squared per Hertz.

B.2.3.5 $S_{10,7}$

As described by[33],[34] the $S_{10,7}$ index is the integrated 26 nm to 34 nm solar irradiance that is measured by the solar extreme-ultraviolet monitor (SEM) instrument on the NASA/ESA Solar and Heliospheric Observatory (SOHO) research satellite. SOHO has an uninterrupted view of the Sun by operating in a halo orbit at the Lagrange Point 1 (L1) on the Earth-Sun line, approximately 1,5 million km from the Earth. SEM was built and is operated by University of Southern California's (USC) Space Science Center (SSC) PI team[32]. Space Environment Technologies (SET) provides an operational backup system called APEX for the SEM data processing as well as creating and distributing the $S_{10,7}$. SOHO was launched on December 2, 1995; and SEM has been making observations since December 16, 1995. The SEM instrument measures the 26 nm to 34 nm solar EUV emission with 15 s time resolution in this first order broadband wavelength range.

The $S_{10,7}$ index is an activity indicator of the integrated 26 nm to 34 nm solar emission and is created by first normalizing the data, then converting it to sfu via a first-degree polynomial fit with $F_{10,7}$. Spikes from abnormal flares and missing data were excluded from the fitting vectors. Normalization is achieved for the 1 AU adjusted epoch values, denoted as $S_{SOHO\_SEM26\_34}$, by division of a mean value over a time frame common to multiple datasets. The mean value = 1,995 5×10^{10} photons cm^{-2} s^{-1}. The common time frame is December 16, 1995 to June 12, 2005, which is generally equivalent to solar cycle 23. The resulting index is called $S_{10,7}$.

In addition to this basic derivation, corrections to $S_{10,7}$ are made as follows. The originally released version of $S_{10,7}$ (v1.8) ranged from January 1, 1996 to December 30, 2005. In versions 3.0–3.9 used by JB2008, the $S_{10,7}$ values between those dates are the original ones derived in v1.8. However, in versions 3.0–3.9 after June 12, 2005, a slight long-term trend was removed to ensure that similar values at the minima of solar cycles 22 and 23 were achieved. For JB2008, ($S_{10,7}$ values v4.0 and higher) a new derivation was completed as given in Formula (B.3); and there may be slight differences of < 0,5 % compared to earlier versions of $S_{10,7}$. Figure B.1 shows $S_{10,7}$ and S_{81} (81-day centred smoothed) values (v4.0) for solar cycle 23 from January 1, 1997 to January 1, 2009.

Daily updated values are found at the JB2008 menu link https://spacewx.com/jb2008/ on the SET website.

$$S_{10,7} = (-2{,}901\ 93) + (118{,}512) \times (S_{\text{SOHO\_SEM26\_34}}/1{,}995\ 5 \times 10^{10}) \quad \text{(B.3)}$$

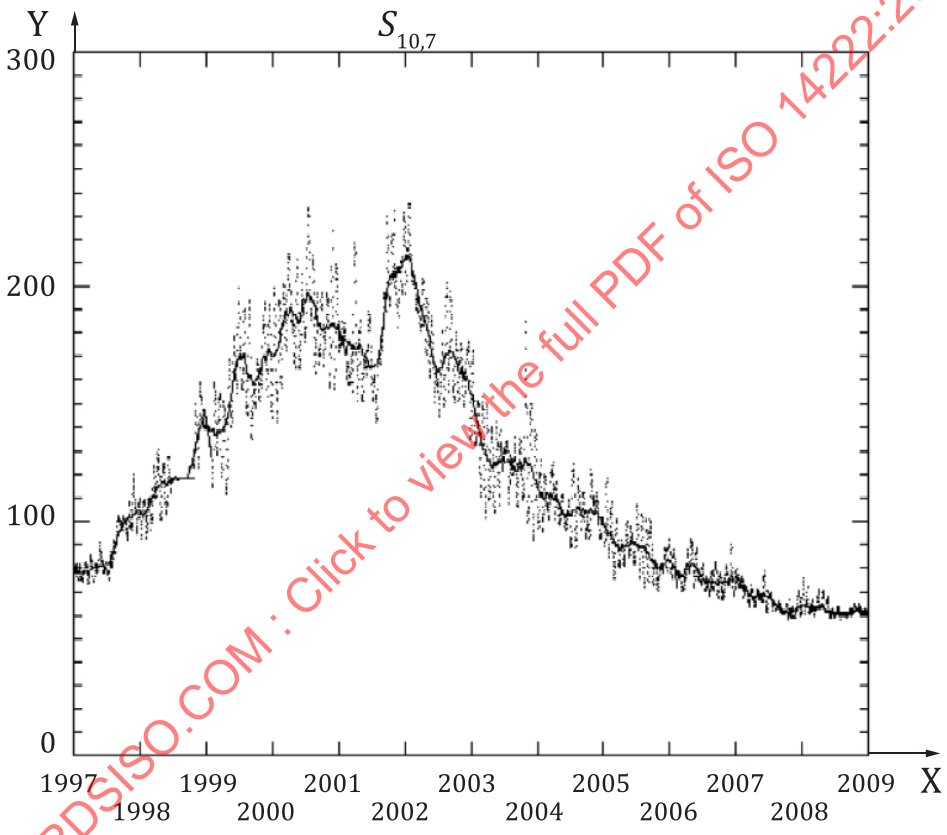

Key

X year

Y sfu

Figure B.1 — $S_{10,7}$(v4.0) daily and 81-day smoothed values for use by the JB2008 model from January 1, 1997 to January 1, 2009

Chromospheric He II at 30,4 nm and coronal Fe XV at 28,4 nm dominate the broadband SEM 26 nm to 34 nm irradiances but that bandpass includes contributions from other chromospheric, transition region, and coronal lines. It is noted that when the SOHO SEM and TIMED SEE 26 nm to 34 nm integrated data are compared, there are differences in the time series particularly during active solar conditions. It is possible that the SOHO SEM measurements are slightly contaminated with 2nd order emissions from the coronal 17,1 nm Fe IX line that have not been removed; however, this topic needs further investigation. The energy in this bandpass principally comes from solar active regions, plage, and network. Once the photons reach the Earth, they are deposited (absorbed) in the terrestrial thermosphere mostly by atomic oxygen above 200 km. The daily $S_{10,7}$ index and its 81-day running

centre-smoothed values, S_{81}, with a 1-day lag (the best correlation with satellite density residuals) as described in Reference [3] are used.

It is inferred that the 1-day lag is consistent with the average atomic oxygen thermal conduction timescale in the thermosphere above 180 km.

B.2.3.6 $M_{10,7}$

The development of the $M_{10,7}$ index is described in Reference [34]. It is derived from the Mg II core-to-wing ratio (cwr) that originated from the NOAA series operational satellites, e.g. NOAA-16, -17, -18, which host the solar backscatter ultraviolet (SBUV) spectrometer[35],[36]. This instrument has the objective of monitoring ozone in the Earth's lower atmosphere and, secondarily, making solar UV measurements. In its discrete operating mode, a diffuser screen is placed in front of the instrument's aperture in order to scatter solar middle ultraviolet (MUV) radiation near 280 nm into the instrument. Although the NOAA data are from operational satellites, the SORCE/SOLSTICE and ERS-2/GOME research satellites also make the Mg II cwr measurements.

On the ground, the Mg II core-to-wing ratio (cwr) is calculated between the variable lines and nearly non-varying wings. The result is a measure of chromospheric and some photospheric solar active region activity is referred to as the Mg II cwr and is provided daily by NOAA Space Weather Prediction Center (SWPC) as well as Space Environment Technologies (SET).

The ratio is an especially good proxy for some solar FUV and EUV emissions and it can represent very well the photospheric and lower chromospheric solar FUV Schumann-Runge Continuum emission. The daily Mg II cwr is used in a linear regression with $F_{10,7}$ to derive the $M_{10,7}$ index for reporting in $F_{10,7}$ units and with a 5-day lag.

The 280 nm solar spectral band contains photospheric continuum and chromospheric line emissions. The Mg II *h* and *k* lines at 279,56 nm and 280,27 nm, respectively, are chromospheric in origin while the weakly varying wings or continuum longward and shortward of the core line emission are photospheric in origin. The instruments from all satellites observe both features. On the ground, the ratio of the Mg II variable core lines to the nearly non-varying wings is calculated. The result is mostly a measure of chromospheric solar active region emission that is theoretically independent of instrument sensitivity change through time. However, long-term changes can occur in the index if instrument wavelength calibrations change in-flight or the solar incidence angle into the instrument changes. The daily Mg II core-to-wing ratio (cwr), described by Reference [36] has historically been provided through the NOAA Space Weather Prediction Center (SWPC). It is likely, however, that the index values at NOAA SWPC are presently uncorrected. SET has developed and provides a corrected, operational Mg II cwr data product (MgII*) available at the Products menu link of https://spacewx.com/current-data/ that uses the NOAA-16, –17, –18, SORCE/SOLSTICE, and ERS-2/GOME data sources.

The detailed processing of the MgII* product is described by Reference [37]. The NOAA data come directly through NOAA NESDIS and SET uses the DeLand algorithm[38],[39] to create the index.

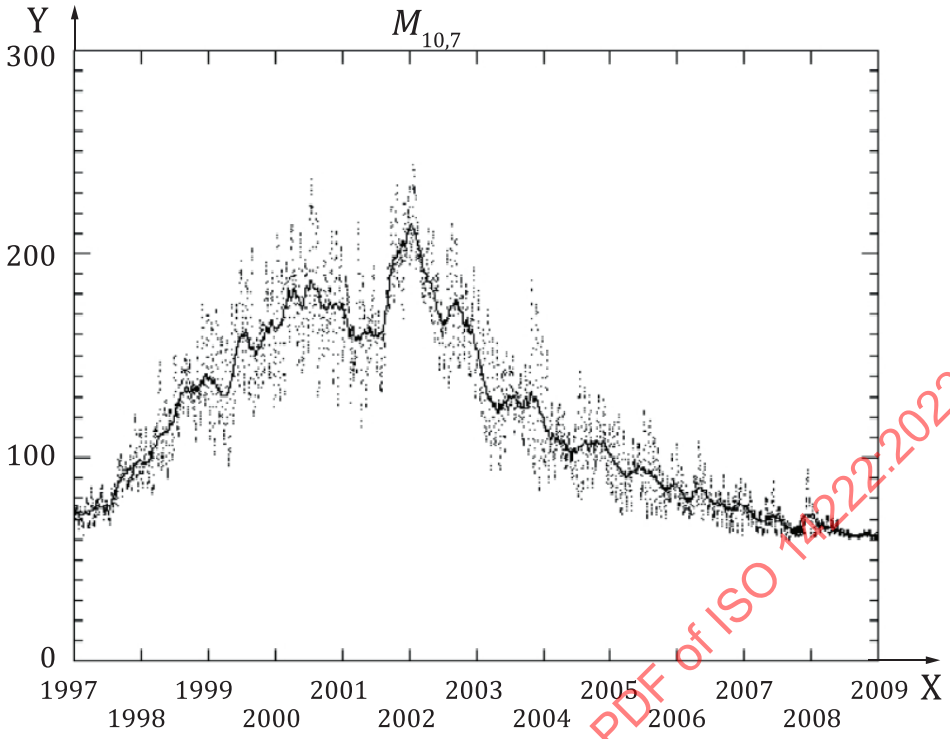

Key

X year

Y sfu

Figure B.2 — $M_{10,7}$ (v4.0) daily and 81-day smoothed values for use by the JB2008 model from January 1, 1997 to January 1, 2009

The Mg II cwr is an especially good proxy for some solar FUV and EUV emissions. It well represents photospheric and lower chromospheric solar FUV Schumann-Runge continuum emission near 160 nm that maps into lower thermosphere heating due to O_2 photodissociation[40]. Since a 160 nm solar FUV emission photosphere index is not produced operationally, the MgII* proxy is used and modified into the $M_{10,7}$ index for comparison with the other solar indices. This derivation is performed in the following manner. A relationship between the long-term (multiple solar cycle) daily MgII* and $F_{10,7}$ is created by making a first-degree polynomial fit to produce a coefficient set that can translate the index into sfu. The result is $M^*_{10,7}$. Next, a correction is added for the decline of solar cycle 23 to account for NOAA 16 instrument degradation that may be related to its diffuser screen illumination geometry changing with time; this cause is unconfirmed. The correction is accomplished by using another first-degree polynomial fit between a trend ratio and day number starting 2448542.0 JD (October 12, 1991 12:00 UT) near the peak of solar cycle 22. The trend ratio is formed from the 365-day centre-smoothed $M^*_{10,7}$ divided by the 365-day centre-smoothed $F_{10,7}$. Formula (B.4) is the final v4.0 formulation of the $M_{10,7}$ index, shown in Figure B.2. The derived $M_{10,7}$ index is reported in sfu, i.e. $F_{10,7}$ units with a lower threshold minimum value set to 60. There may be slight differences of up to 1 % compared to earlier versions of $M_{10,7}$.

$$M_{10,7} = [-2\ 107{,}618\ 6 + (8\ 203{,}053\ 7) \times (r_{MgII})] + [(M^*_{10,7}) \times (1{,}289\ 058\ 9 + (-8{,}377\ 723\ 5 \times 10^{-5}) \times x - 1)] \quad \text{(B.4)}$$

Where r_{MgII} is the MgII core to wing ratio as compiled by SET[37].

NOTE MgII* is commonly used in the industry for r_{MgII}.

The day number x = 0, 1, 2, ... with x = 0 equivalent to starting on 2448542.0 JD.

Figure B.2 shows the $M_{10,7}$ index during solar cycle 23 from January 1, 1997 to January 1, 2009.

The daily $M_{10,7}$ and its 81-day running centre-smoothed values, M_{81}, are used with a 2-day lag in JB2008 as a proxy for the Schumann-Runge continuum FUV emission[3]. Originally, the JB2008 model, which did not use $Y_{10,7}$, had a lag time for $M_{10,7}$ of 5 days since the index was incorporating a combination of lag times from several energy transfer processes in the lower thermosphere to the mesopause. However, with the addition of the lower altitude (85 km to 100 km) relevant $Y_{10,7}$ index, a shorter lag time was appropriate for $M_{10,7}$, which represents O_2 photodissociation, recombination, conduction and transport processes at the 95 km to 110 km level. It is inferred that the 2-day lag is consistent with the average molecular oxygen dissociation and thermal conduction timescale in the thermosphere above 95 km, although eddy and turbulent conduction processes may play a role.

B.2.3.7 $Y_{10,7}$

The $XL_{10,7}$ index was developed as a candidate index for the JB2006 model[34] but was unused. While developing the JB2008 model, it was determined that a thermospheric energy contribution to satellite drag from the 80 km to 95 km region was significantly correlated with the composite $XL_{10,7}$ solar index.

Solar X-rays in the 0,1 nm to 0,8 nm wavelength range come from the cool and hot corona and are typically a combination of both very bright solar active region background that varies slowly (days to months) plus flares that vary rapidly (minutes to hours), respectively. The photons arriving at Earth are absorbed in the lower thermosphere to mesopause and (85 km to 100 km) by molecular oxygen (O_2) and molecular nitrogen (N_2) where they ionize those neutral constituents to create the ionospheric D-region.

The X-ray spectrometer (XRS) instrument is part of the instrument package on the GOES series operational spacecraft. The GOES/XRS provides the historical through current epoch 0,1 nm to 0,8 nm solar X-ray emission data with a 1 min cadence and as low as 5 min latency. These data, which are particularly useful for flare detection, are continuously reported by NOAA SWPC at their website of https://www.swpc.noaa.gov/.

The GOES/XRS 0,1 nm to 0,8 nm data was used by Reference [41] to develop an index of the solar X-ray active region background, without the flare component, for operational use. This is called the X_{b10} index and is used to represent the daily energy that is deposited into the mesosphere and lower thermosphere.

While the 0,1 nm to 0,8 nm X-rays are a major energy source in these atmospheric regions during high solar activity, they relinquish their dominance to another emission that reaches the same optical depth, i.e. the competing hydrogen (H) Lyman Alpha (Lyman-α) emission that is the major energy source in this atmosphere region during moderate and low solar activity. Lyman-α is created in the solar upper chromosphere and transition region and demarcates the EUV from the FUV spectral regions. It is formed primarily in solar active regions, plage and network; the photons, arriving at Earth, are absorbed in the mesosphere and lower thermosphere where they dissociate nitric oxide (NO) and participate in water (H_2O) chemistry. Lyman-α is regularly observed by the SOLSTICE instrument on the UARS and SORCE satellites as well as by the SEE instrument on TIMED[42].